# L'AQUILA EARTHQUAKE NEAR-FAULT ACCELEROMETER REGISTRATIONS SEISMIC DEMAND IN TERMS OF DAMAGE INDEXES

Bruno Palazzo, Massimiliano De Iuliis

palazzo@unisa.it, mdeiuliis@unisa.it

*Department of Civil Engineering, University of Salerno, Italy*

In this report, an experimental numerical study aiming to evaluate the seismic demand on inelastic SDOF system (iSDOF) in terms of damage indexes for near-fault recorded accelerometric signals from "L'Aquila earthquake" (date 06/04/2009 – 1.32AM UTC – Local Magnitude 5.8) is presented.

In table 1 the corrected horizontal acceleration components taken into consideration are listed.

Table 1: Recorded accelerograms being considered

| Registration code | Station | Site | Soil profile | Topography factor | Epicentre distance (Km) |
|---|---|---|---|---|---|
| FA030 | AQG | Colle dei Grilli | type B | $S_T$=1,1 | 4,3 |
| GX066 | AQX | Aterno Valley | type B | $S_T$=1,0 | 4,8 |
| AM043 | AQK | Aquila Parking | type C | $S_T$=1,1 | 5,6 |
| CU104 | AQA | Aterno River | type B | $S_T$=1,0 | 5,8 |

Soil parameters have been preliminarily estimated (1) from data available from the ITACA database (2) on accelerometric RAN network (3) and from the geographical database available from the Regione Abruzzo (4).

The model adopted to represent the non-linear behaviour of the SDOF systems is the well-known elastic-perfectly plastic model, for each accelerometric component, different analyses have been carried out to characterise main aspects of the L'Aquila Earthquake. In particular, Park and Ang (PA) and low-cycle fatigue (LF) damage indexes have been evaluated on varying the iSDOF mechanical parameters: resistance level, monotonic ductility and viscous damping. The choice of the indexes to be considered has been carried out having

the aim to relate their values with the damage level of real structures, in this within both *PA* and *LF* indexes are widely adopted within the scientific community and different works exist which trying to correlate their value with observable damage level (5). Moreover, technical literature often reports the values of these damage indexes for most of the main recorded earthquake signal in the last 20 years, including near-fault events, allowing for a straightforward and useful comparison.

It is worth to state that the resistance level in the numerical analysis, throughout the present report, is obtained by scaling, through a reduction factor, the elastic demand spectra according to the new Italian seismic code (NTC2008) (6) for ordinary constructions (reference period $V_R$=50 yrs). Therefore reduction factors are not evaluated with respect to the elastic spectra of the incoming seismic excitations, the main purpose of this work is, in fact, to estimate the effect of the L'Aquila earthquake on ideal structures designed according to the new Italian provisions

- ***CONSIDERED DAMAGE INDEXES***

The Park and Ang damage index (7,8), as well known, is defined by the following equation:

$$PA = \frac{x_{\max}}{x_{u,mon}} + \beta \frac{E_h}{F_y \cdot x_{u,mon}} = \frac{\mu_S + \beta(\mu_e - 1)}{\mu_{u,mon}} \tag{1}$$

which main idea is that damage is related with both cinematic and hysteretic ductility demand, with the coefficient $\beta$ having the meaning of a "degradation" parameter and weighting, in terms of damage, the ratio between displacement and energy demand. In this report $\beta = 0.15$ has been adopted, in accordance with the mean value obtains from different authors (9,10). A consolidate literature also relates PA index values to structural damage level (5,11,12), table 2 categorizes the observed damage into five levels pointed out the correspondent PA index, moreover in figure 1, these levels are correlated with three performance levels.

In this report two values are considered for the PA index, $PA = 1.0$ and $PA = 0.4$, the first one corresponds to the structural collapse, the other one is the threshold value between moderate and severe damage, it can be considered as a numerical limit to avoid being exceed in order to guarantee the cost effectiveness in repairing the structural system. The aim is to estimate the minimal iSDOF resource in terms of both resistance and monotonic ductility to avoid collapse ( $PA = 1.0$ ) or severe damage ( $PA = 0.4$ ) in the structural system.

Table 2: Park and Ang damage classification levels

| PA index values | Observed structural damage |
|---|---|
| $PA < 0.1$ | No damage or localized cracking |
| $0.1 \le PA < 0.25$ | Minor damage |
| $0.25 \le PA < 0.4$ | Moderate damage |
| $0.4 \le PA < 1.0$ | Severe damage |
| $PA > 1.0$ | Collapse |

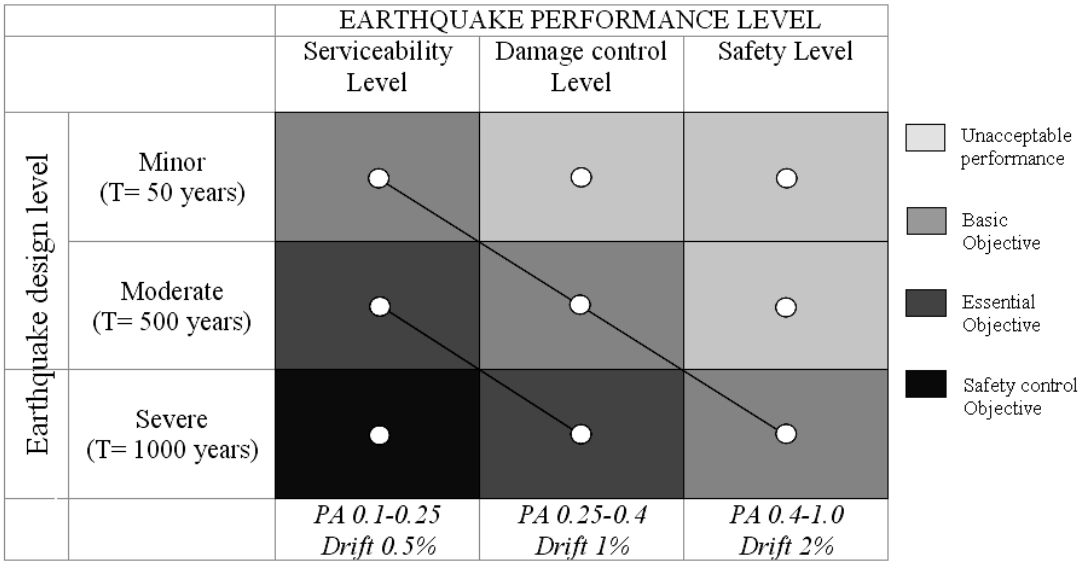


Figure 1: Performance Based Seismic design matrix and PA damage index values

Moving on the low-cycle fatigue damage index (13, 14), it is defined as:

$$LF = \sum_{i=1}^{n} \left( \frac{\mu_{S,i} - 1}{\mu_{u,mon} - 1} \right)^{b} \tag{2}$$

where $n$ represents the overall number of plastic cycle, $\mu_{S,i}$ is the demanded cinematic ductility at i-th cycle, $b$ is a constant, which depends on the structural material and typology, the number of different plastic displacements. The value of $b$ significantly affects the value of $LF$ index, it represents a sort of weighting factor to estimate the effect of the single plastic strains on structural damage. According to Banon et al. (15) a conservative value of *1.5* is herein assumed. Due to not reliable technical literature available data to correlate single structural performance to LF damage index value, in this report the single case of structural collapse corresponding to $LF = 1$ is considered.

- ***SEISMIC DEMAND IN TERM OF PARK AND ANG INDEX***

As already stated, the main aim of the present work is to provide more specific information on iSDOF ductility and resistance demand for l'Aquila seismic registrations, in order to obtain pre-assigned structural performance for different resistance levels. In particular, the following numerical analysis has been carried out:

- the Park and Ang damage index, in the case of iSDOF having fixed monotonic ductility ($\mu_{u,mon} = 4$) and different resistant level on varying the damping capacity has been plotted for the considered seismic registrations (Figures 2-25),

- the minimum ductility capacity spectra $\mu_{u,mon}^{\min}$ on varying the iSDOF resistance level to prevent respectively Collapse ($PA = 1.0$) (Figures 26-33) and damage to the structural elements ($PA = 0.4$) (Figures 34-41) are evaluated and plotted.

By examining the results plotted in figure 2-25 it's clear that in the case of very stiff structural system *T=0÷0.2 sec* very high damage level are expected, moreover attention should be paid on structural systems having their fundamental period between 0.2 and 0.7 sec., their estimated damage level can assume values in a wide range. In particular three cases can be distinguished

- iSDOF having high resistance resource ($R_\mu = 2$), in this case Park and Ang index values are compatible with low-moderate damage level, if high viscous damping resource are available, elastic response has been observed

- iSDOF having medium resistance resource ($R_\mu = 4$, which is close to the "B" ductility class in new Italian code), in this condition damage level assumes very different values, from no damage to collapse, depending on the available damping resource

- iSDOF having low resistance resource ($R_\mu = 6$, which is close to the "A" ductility class in new Italian code), in this case structural damage are very severe and, in the most cases, even high damping resource cannot prevent potential collapse of the structural system.

As can be easily observed, Park and Ang damage index values decrease by increasing the fundamental period of the system, which confirms the considered seismic registrations are no dangerous for flexible structures. This results have to be viewed by considering that a fixed monotonic ductility resource ($\mu_{u,mon} = 4$) has been fixed, the effect on varying such parameter can be inferred just analyzed the results showed in figures 26-41, in which is the damping resource to stay unchanged ($\xi = 0.05$) and the seismic demand in terms of monotonic ductility to be evaluated in order to accomplish pre-assigned structural performance levels.

## *AQG Station – FA030 recording – Park & Ang damage index - $\mu_{mon}$=4*

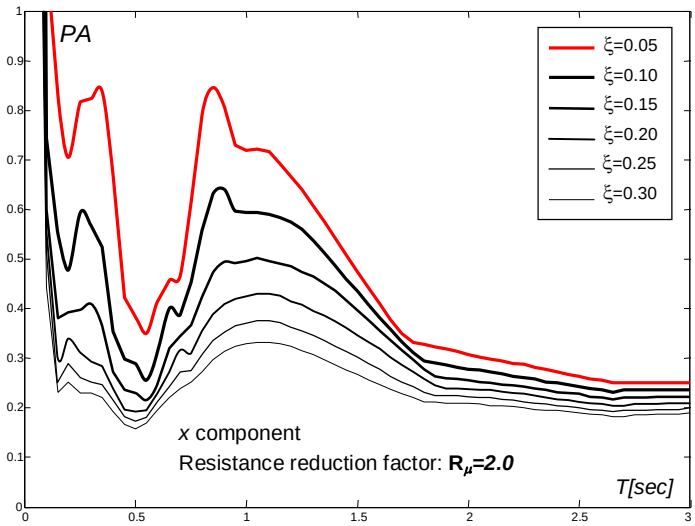


**Figure 2:** *PA* damage index on varying SDOF damping

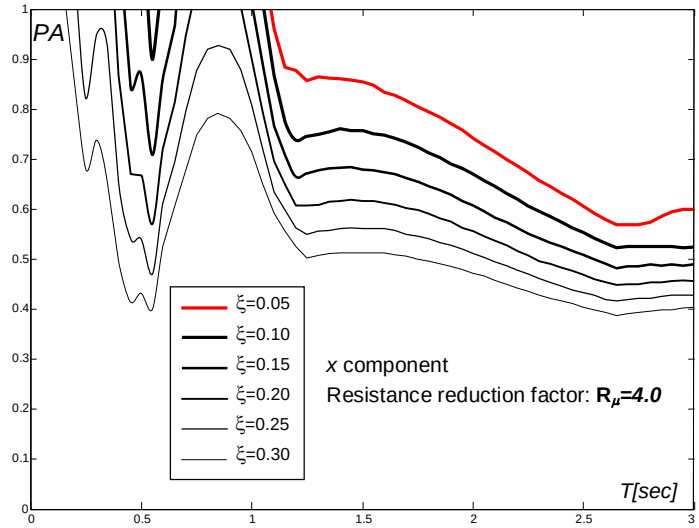


**Figure 3:** *PA* damage index on varying SDOF damping

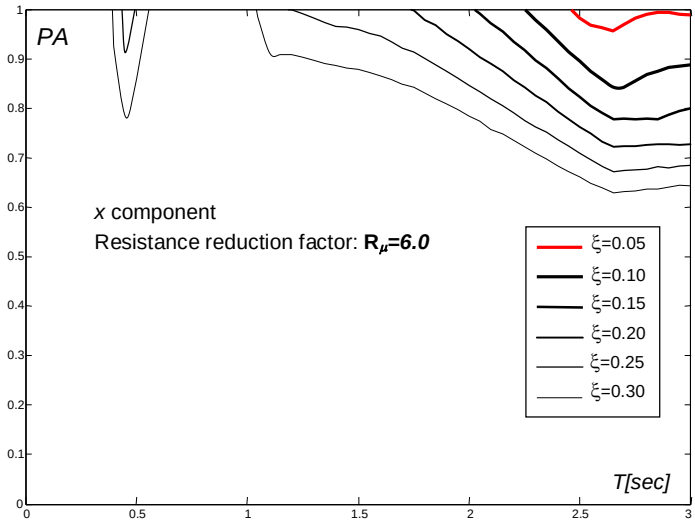


**Figure 4:** *PA* damage index on varying SDOF damping

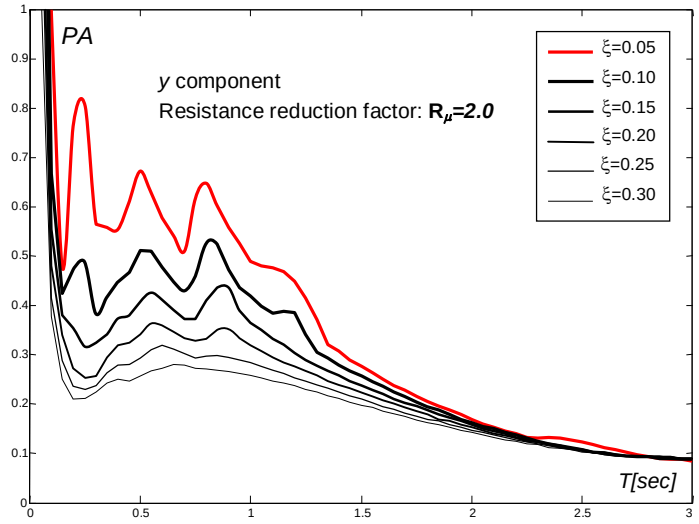


**Figure 5:** *PA* damage index on varying SDOF damping

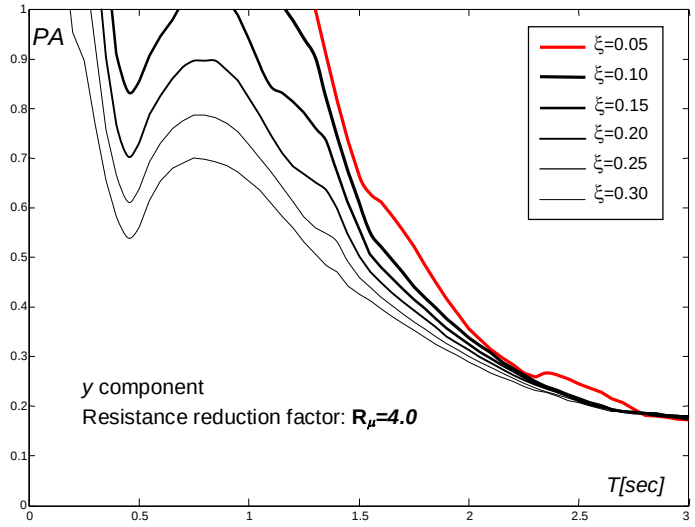


**Figure 6:** *PA* damage index on varying SDOF damping

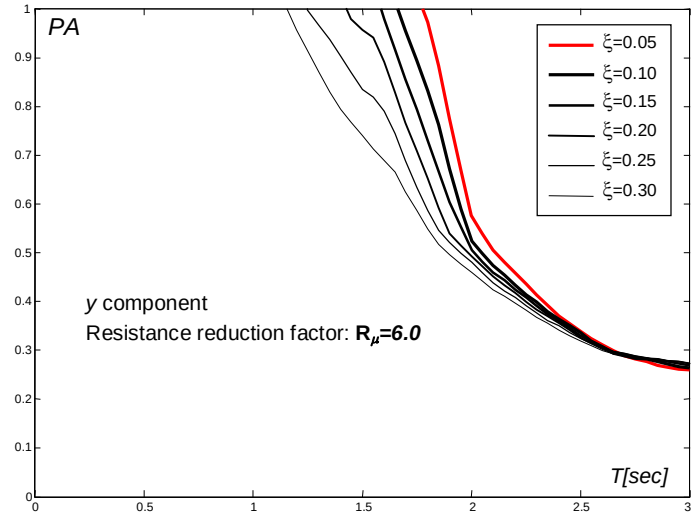


**Figure 7:** *PA* damage index on varying SDOF damping

# *AQX Station – GX066 recording – Park & Ang damage index - $\mu_{mon}$=4*

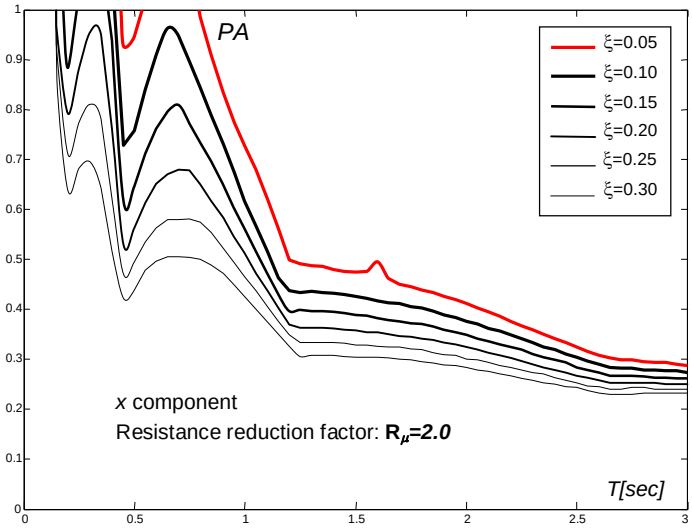


**Figure 8:** *PA* damage index on varying SDOF damping

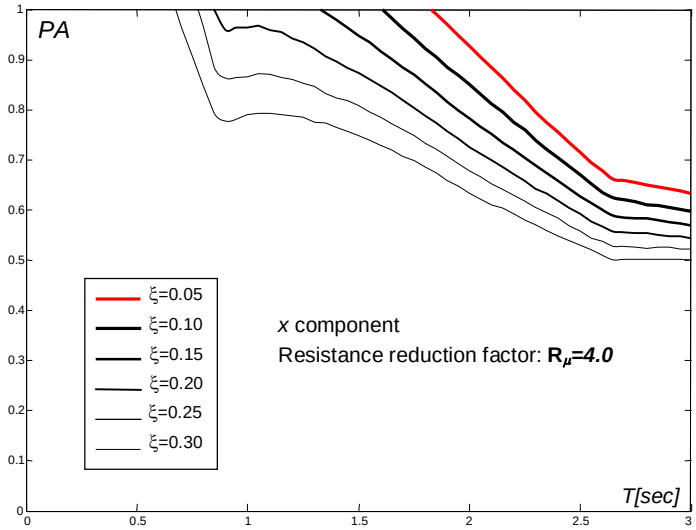


**Figure 9:** *PA* damage index on varying SDOF damping

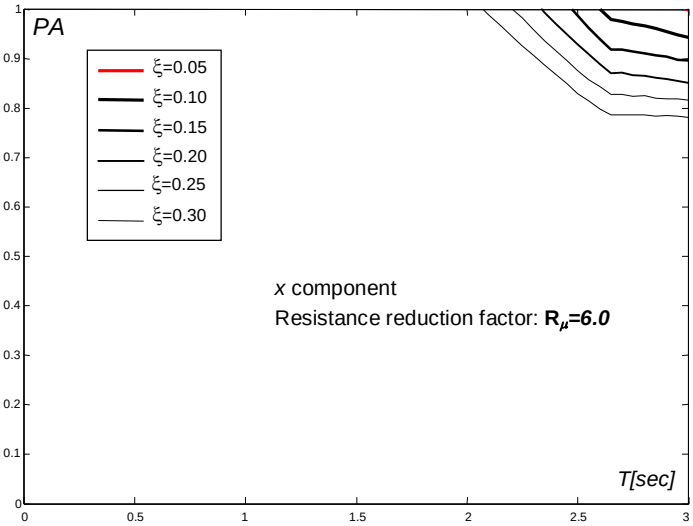


**Figure 10:** *PA* damage index on varying SDOF damping

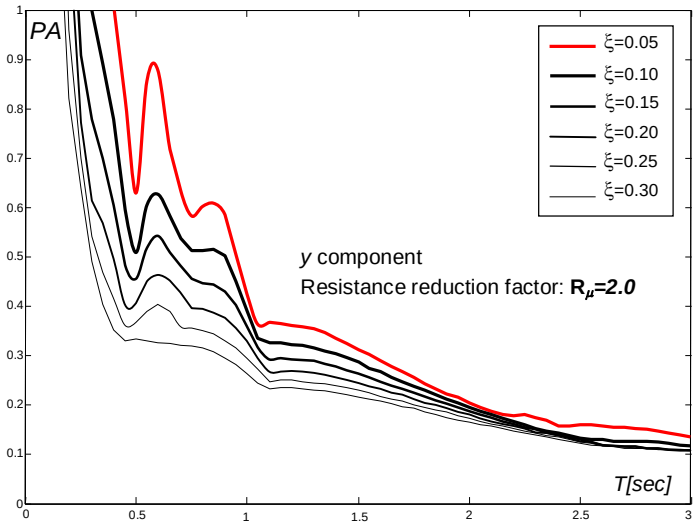


**Figure 11:** *PA* damage index on varying SDOF damping

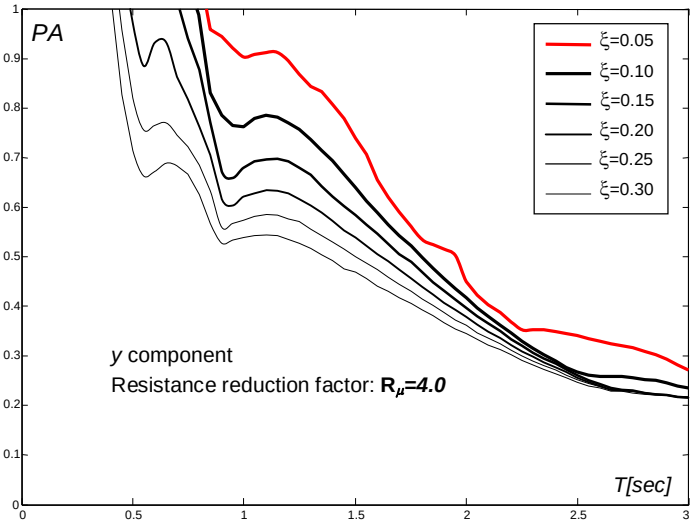


**Figure 12:** *PA* damage index on varying SDOF damping

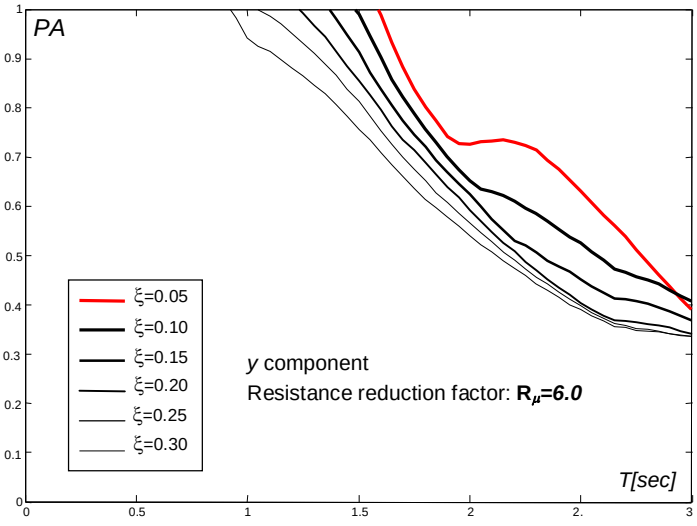


**Figure 13:** *PA* damage index on varying SDOF damping

## *AQK Station – AM043 recording – Park & Ang damage index - $\mu_{mon}$=4*

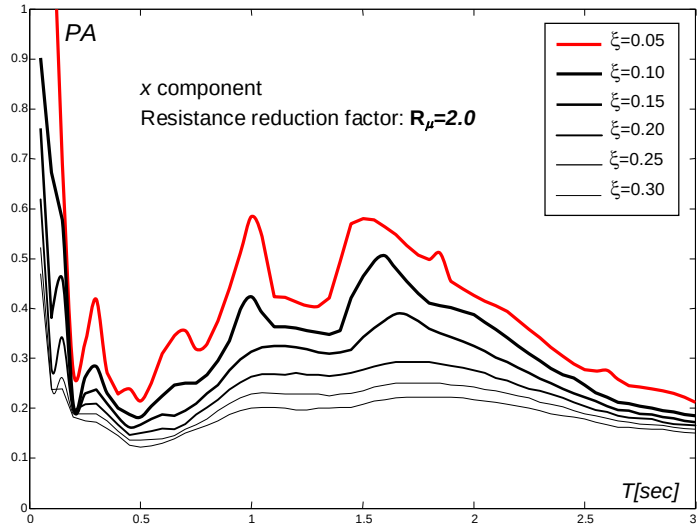


**Figure 14:** *PA* damage index on varying SDOF damping

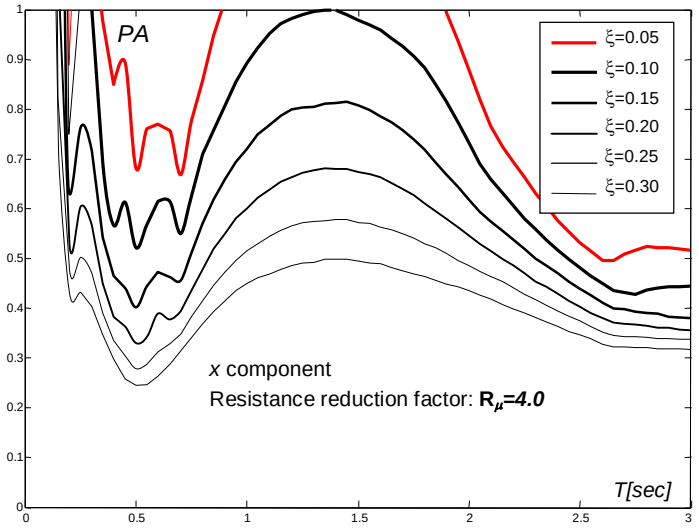


**Figure 15:** *PA* damage index on varying SDOF damping

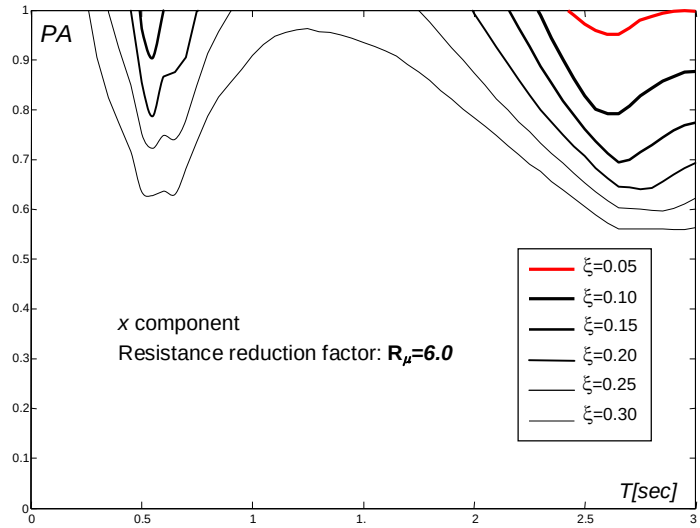


**Figure 16:** *PA* damage index on varying SDOF damping

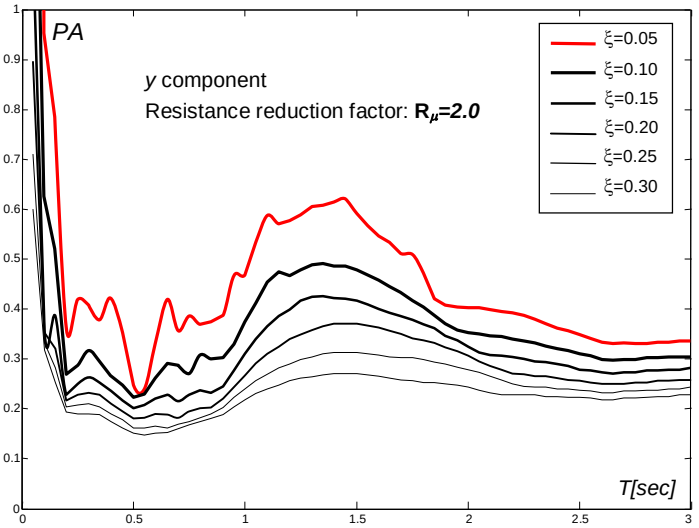


**Figure 17:** *PA* damage index on varying SDOF damping

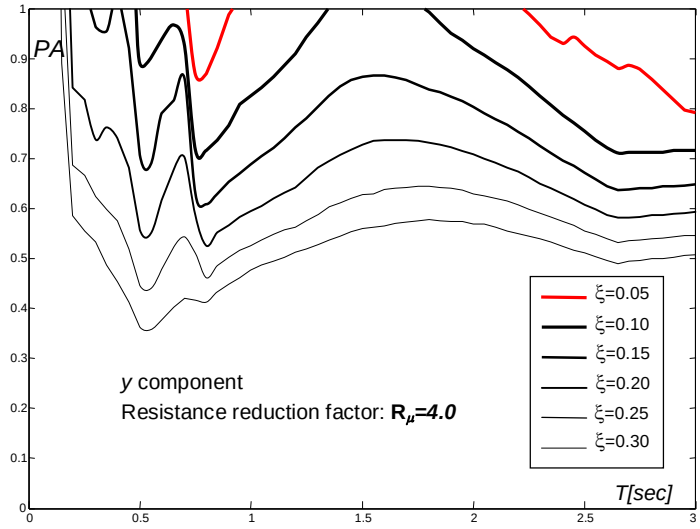


**Figure 18:** *PA* damage index on varying SDOF damping

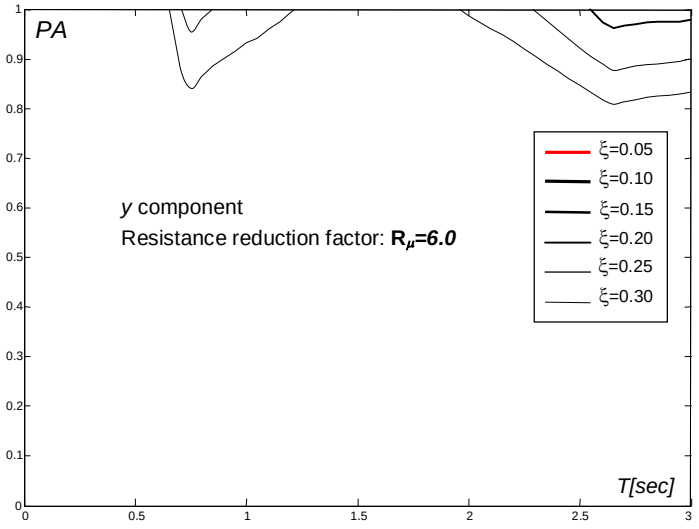


**Figure 19:** *PA* damage index on varying SDOF damping

## *AQA Station – CU104 recording – Park & Ang damage index - $\mu_{mon}$=4*

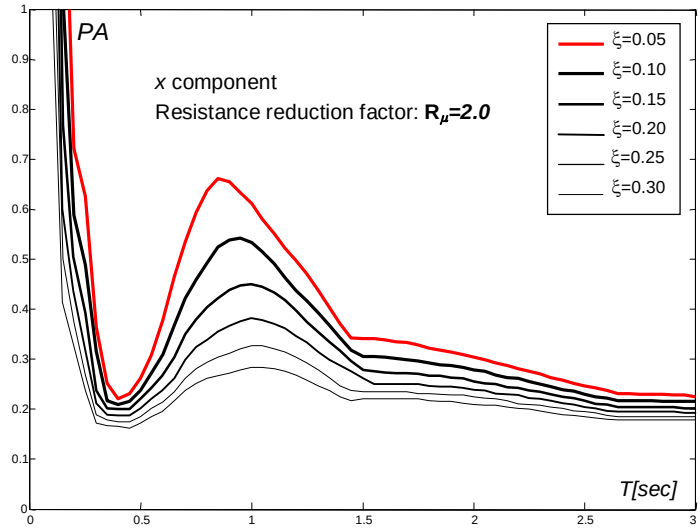


**Figure 20:** *PA* damage index on varying SDOF damping

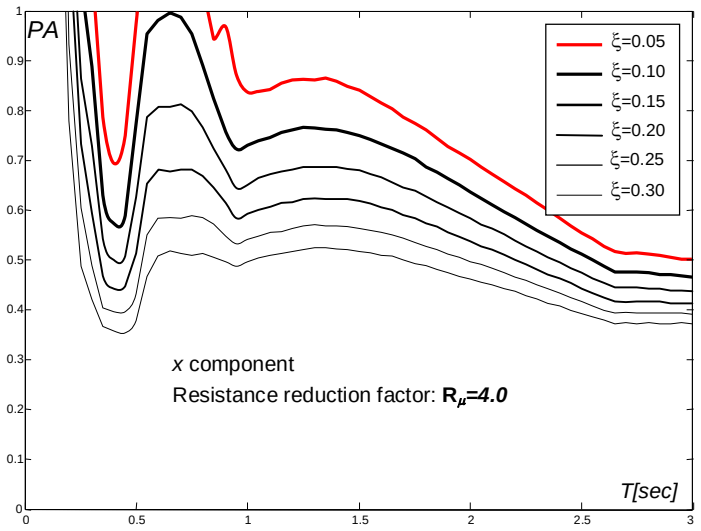


**Figure 21:** *PA* damage index on varying SDOF damping

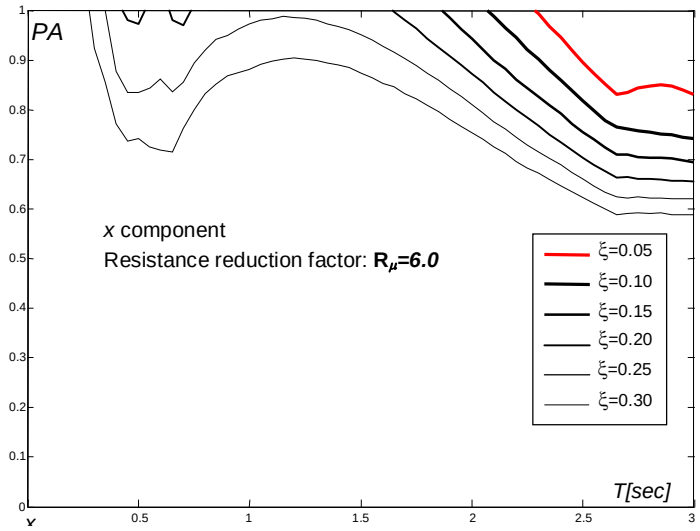


**Figure 22:** *PA* damage index on varying SDOF damping

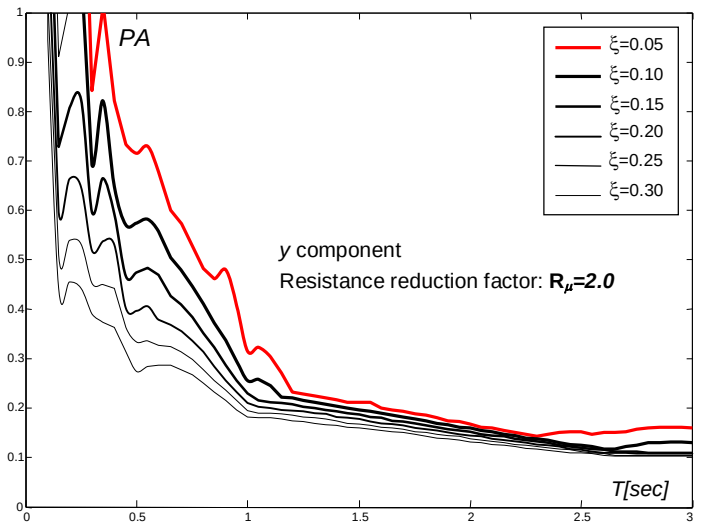


**Figure 23:** *PA* damage index on varying SDOF damping

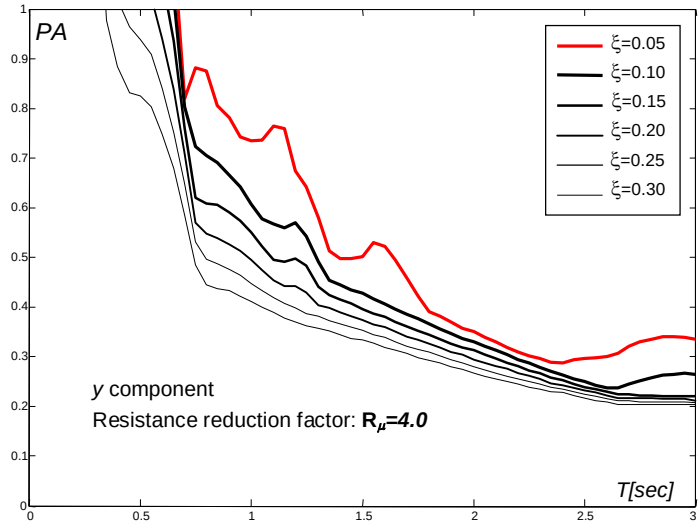


**Figure 24:** *PA* damage index on varying SDOF damping

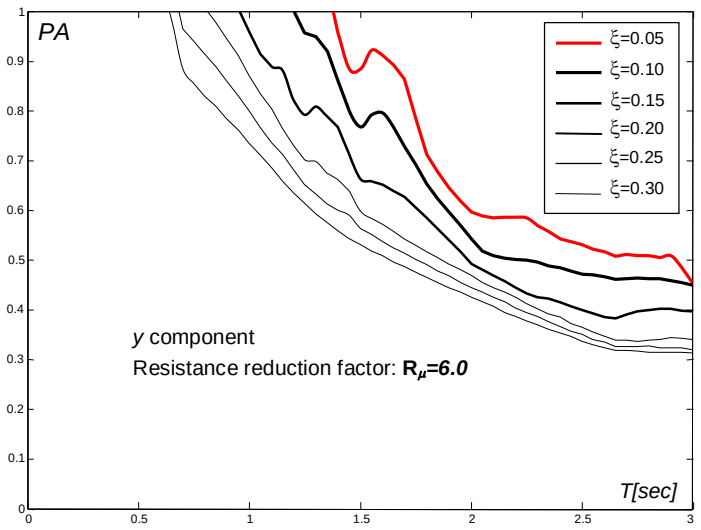


**Figure 25:** *PA* damage index on varying SDOF damping

***AQG Station – FA030 recording – x component***

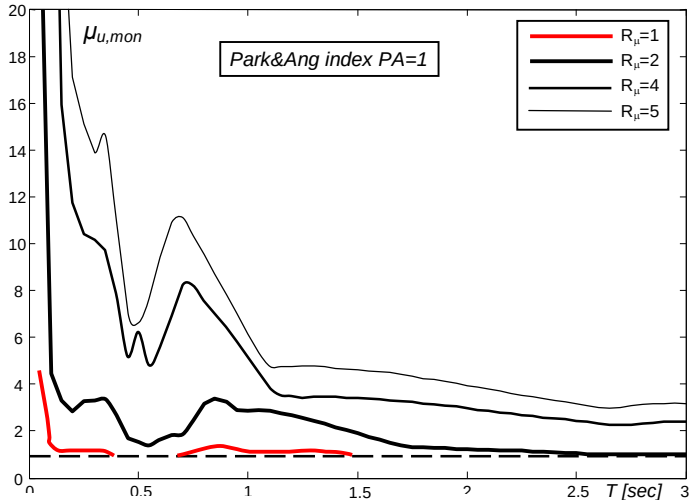


**Figure 26**: Ductility demand spectra for Collapse Limit State (*PA=1.0*)

***AQG Station – FA030 recording – y component***

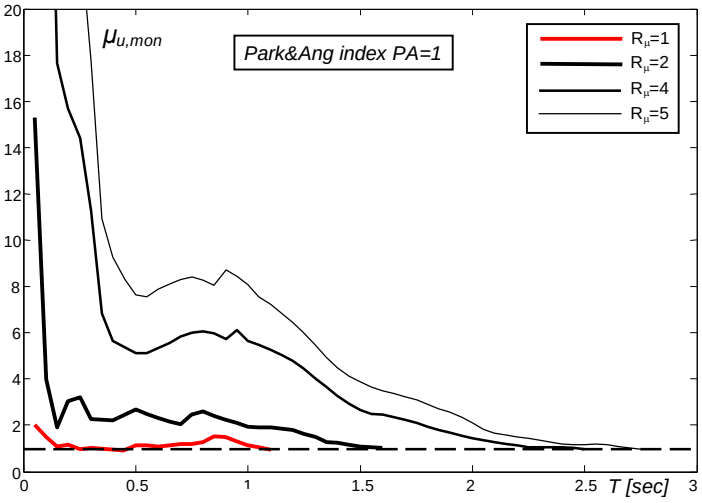


**Figure 27**: Ductility demand spectra for Collapse Limit State (*PA=1.0*)

***AQX Station – GX066 recording – x component***

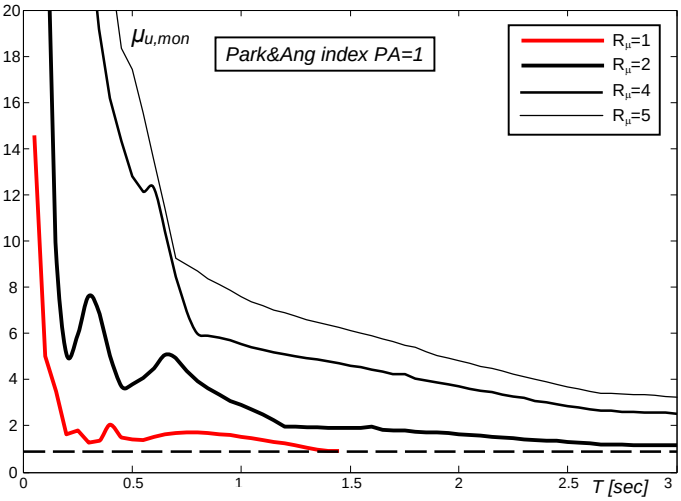


**Figure 28**: Ductility demand spectra for Collapse Limit State (*PA=1.0*)

***AQX Station – GX066 recording – y component***

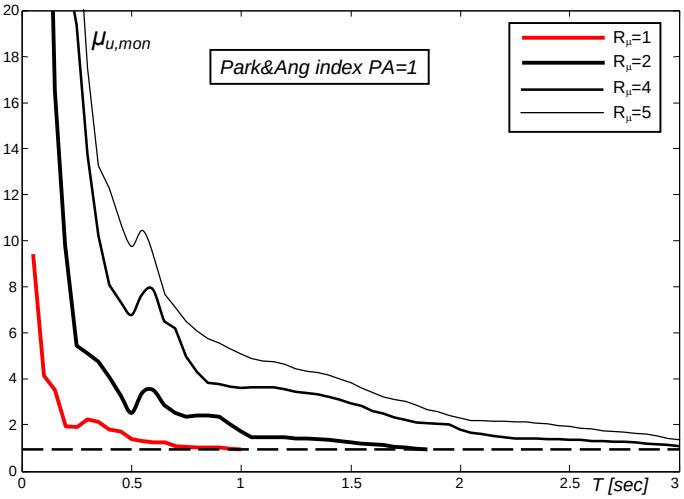


**Figure 29**: Ductility demand spectra for Collapse Limit State (*PA=1.0*)

***AQK Station – AM043 recording – x component***

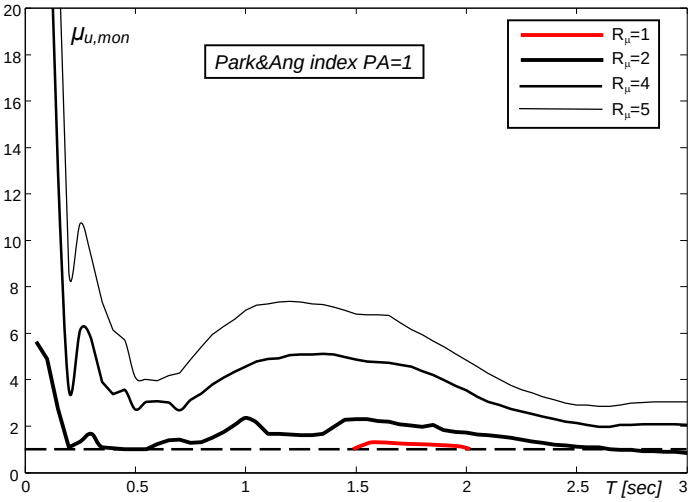


**Figure 30**: Ductility demand spectra for Collapse Limit State (*PA=1.0*)

***AQK Station – AM043 recording – y component***

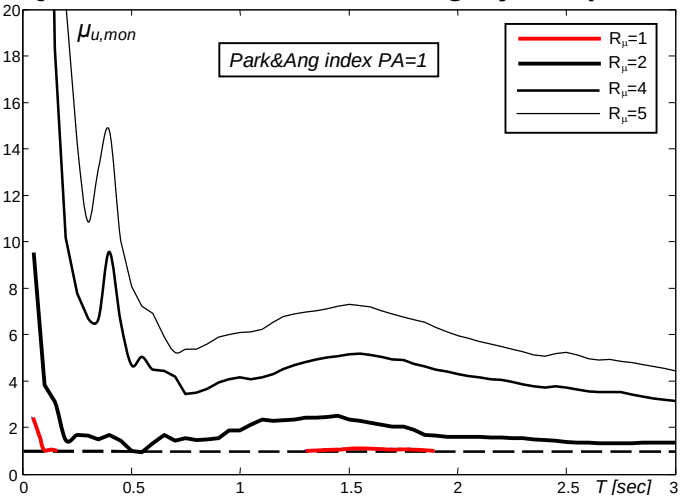


**Figure 31**: Ductility demand spectra for Collapse Limit State (*PA=1.0*)

***AQA Station – CU104 recording – x component***

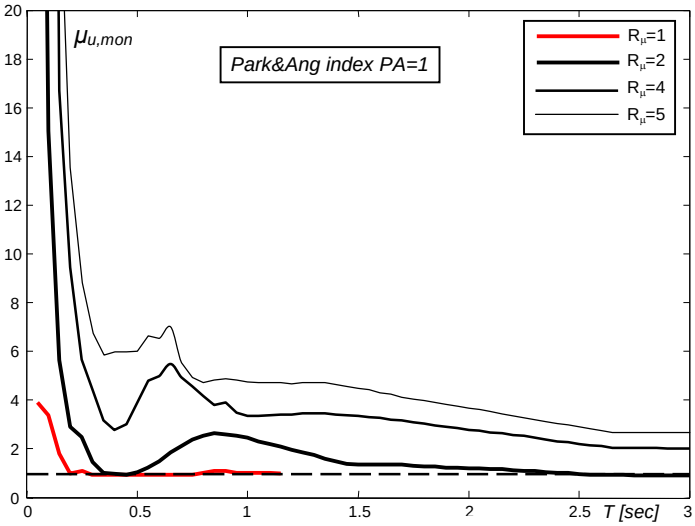


**Figure 32**: Ductility demand spectra for Collapse Limit State (*PA=1.0*)

***AQA Station – CU104 recording – y component***

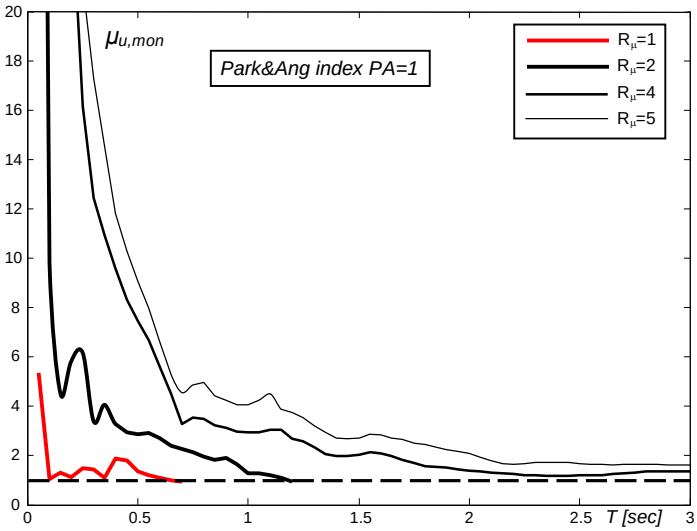


**Figure 33**: Ductility demand spectra for Collapse Limit State (*PA=1.0*)

***AQG Station – FA030 recording – x component***

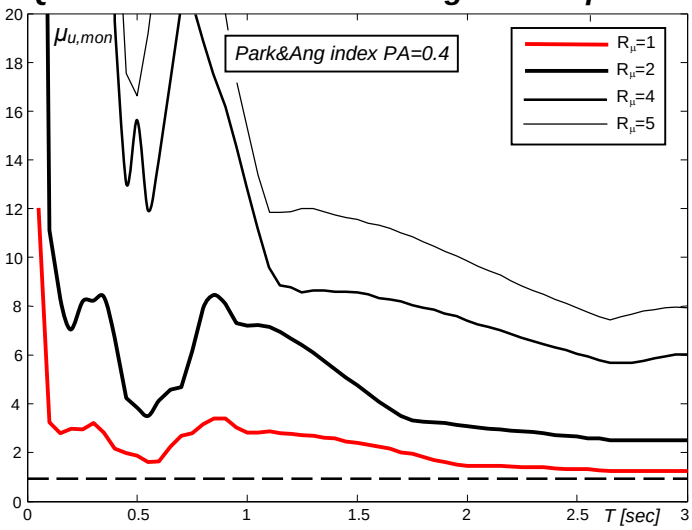


**Figure 34**: Ductility demand spectra for Damage Limit State (*PA=0.4*)

***AQG Station – FA030 recording – y component***

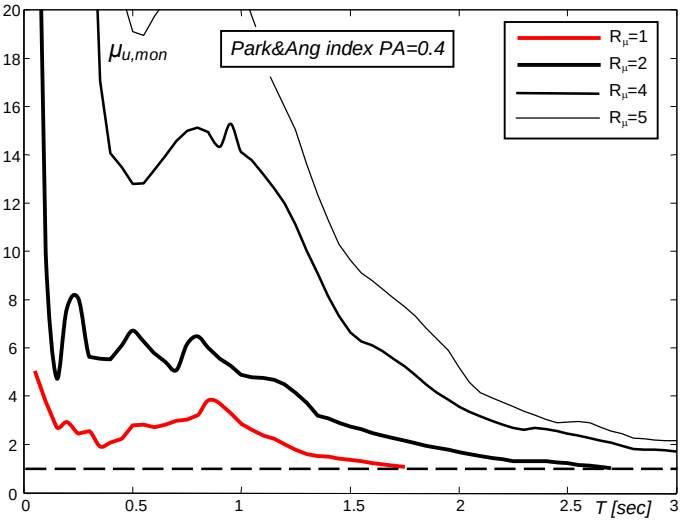


**Figure 35**: Ductility demand spectra for Damage Limit State (*PA=0.4*)

***AQX Station – GX066 recording – x component***

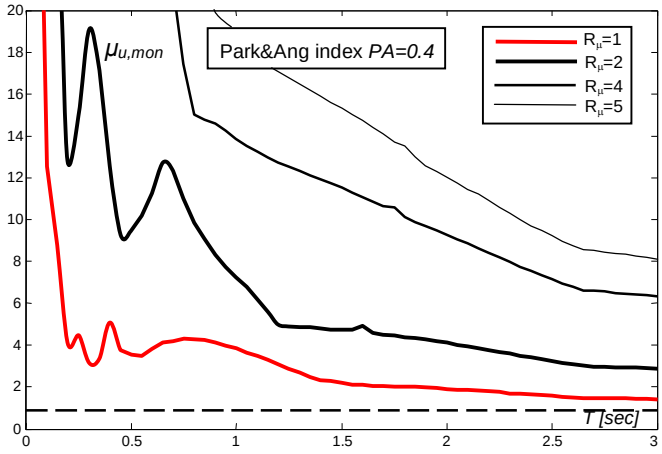


**Figure 36**: Ductility demand spectra for Damage Limit State (*PA=0.4*)

***AQX Station – GX066 recording – y component***

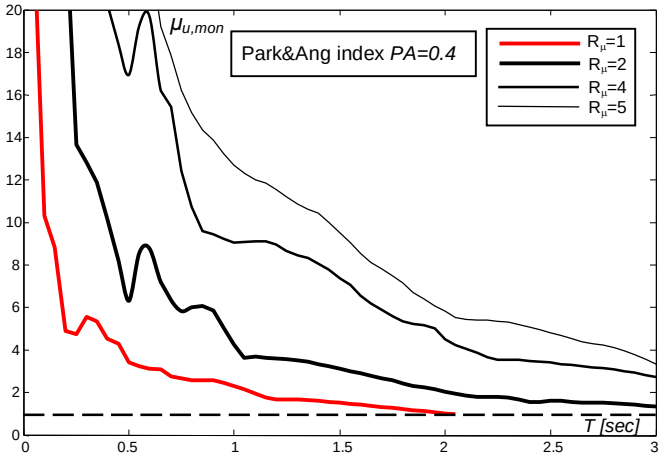


**Figure 37**: Ductility demand spectra for Damage Limit State (*PA=0.4*)

***AQK Station – AM043 recording – x component***

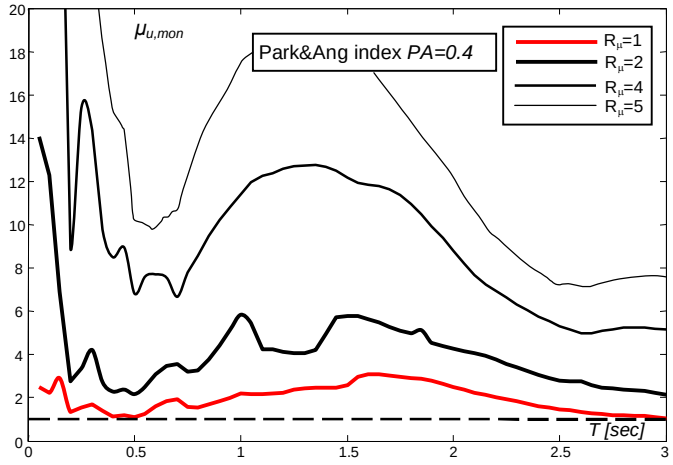


**Figure 38**: Ductility demand spectra for Damage Limit State (*PA=0.4*)

***AQK Station – AM043 recording – y component***

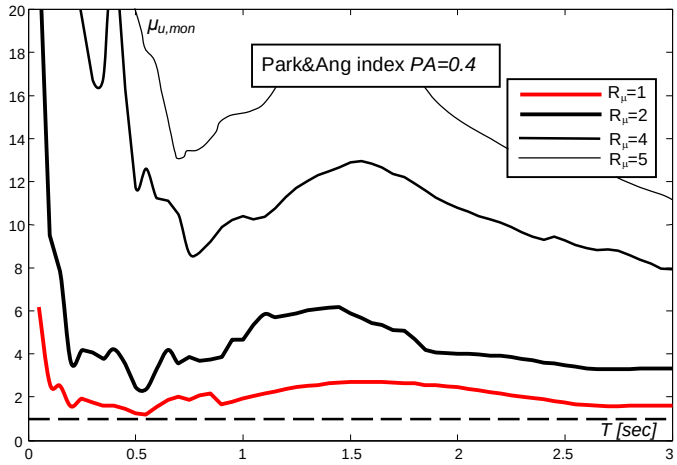


**Figure 39**: Ductility demand spectra for Damage Limit State (*PA=0.4*)

***AQA Station – CU104 recording – x component***

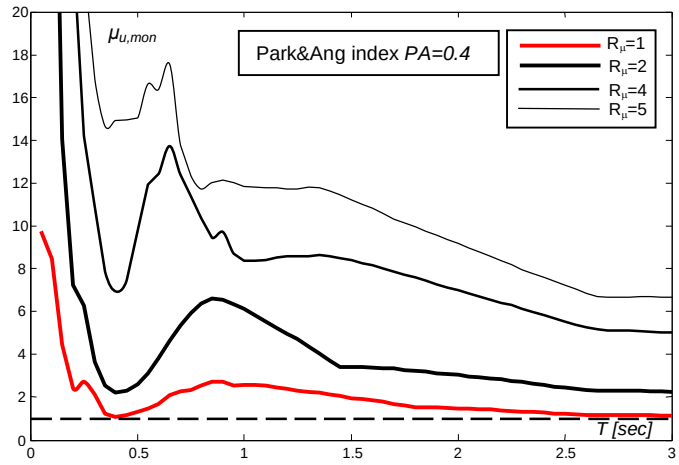


**Figure 40**: Ductility demand spectra for Damage Limit State (*PA=0.4*)

***AQA Station – CU104 recording – y component***

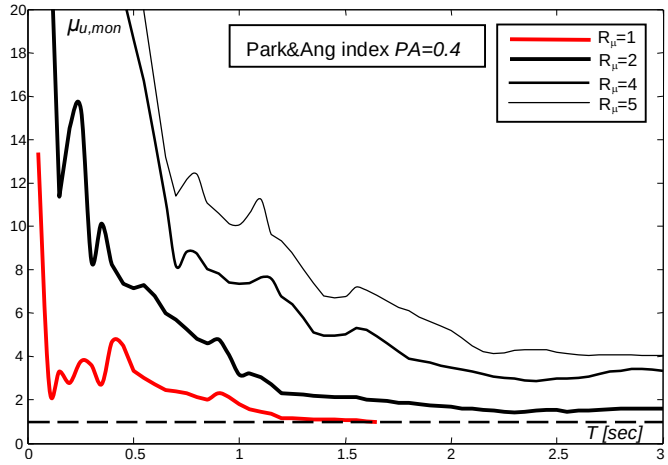


**Figure 41**: Ductility demand spectra for Damage Limit State (*PA=0.4*)

Obtained results show different hazard level from the four near-fault seismic excitations. The most dangerous appears to be the GX066 registration, station AQX, in particular the seismic demand related to the x-component of such recorded accelerogram is well over the inelastic demand described into the new Italian Code. In such case, the collapse limit state can be avoided, if typical monotonic ductility values $\mu_{u,mon} \in [4,6]$ are considered, by providing a resistance level that is half of the elastic spectrum in new Italian Code, $R_\mu = 2$, whereas for both ductility levels considered in that code (low and high ductility classes), values suggested for $R_\mu$ are higher (figure 28). The same accelerogram demands for resistance similar to new code elastic spectra in order to avoid severe damage in the structural system (figure 36). The y-component, recorded by the same station, have also high seismic demand, slightly lower than the other component (figure 29, 37), it's remarkable that the very high seismic demand from these seismic excitations is concentrated on low vibration periods, in fact it drastically reduces when $T > 0.7 \div 1\text{sec}$.

Seismic registration FA030, station AQG, also is characterized by a considerable seismic demand. For both component resistance level obtained by applying a reduction factor $R_\mu = 3$ to the new Italian code elastic spectra allows to avoid collapse of a system having typical monotonic ductility and fundamental period lower than 1 second (figure 26,27). With respect to the damage limit state, y-component appears to be more dangerous for stiff system than x-component, however the latter presents demands peak for structural system having their periods in the range 0.6-1 sec. (figure 34,35).

The other two considered near-fault registrations have seismic demands closest to the Italian new code provisions, the CU104 registration, station AQA, doesn't lead the system toward collapse when resistance and ductility resources compatible with the design rules stated by the DM 14.01.08 are correctly applied, however the damage limit state is not guarantee if high resistance values are not provided ($R_\mu \leq 2$) . It is worth to note that also in the case of flexible structures the x-component of this seismic registration demands for high values of the monotonic ductility. Finally, the AM043 registration, AQK station, is surely the less demanding seismic excitations within the considered set, with a resistance value characterized by a reduction value equal to $R_\mu = 3$ both the collapse and the damage limit state are accomplished practically all over the considered period range. The amplification effect on high period for this accelerogram, already proof in previous studies (Ref), is observable too, in particular in the fundamental period range $T \in [1\text{sec}, 2\text{sec}]$ the seismic demand significantly increase, leading, however, to a severe damage state just for very low resistance level.

- ***SEISMIC DEMAND IN TERM OF LOW-CYCLE FATIGUE INDEX***

Similar analysis concerning have been also carried out by considering the low-cycle fatigue index (LF). In particular numerical analysis have been performed in order to evaluate:

- the low-cycle fatigue index, in the case of iSDOF having fixed monotonic ductility ($\mu_{u,mon} = 4$) and different resistant level on varying the damping capacity for the considered seismic registrations (Figures 42-65),
- the minimum ductility capacity spectra $\mu_{u,mon}^{\min}$ on varying the iSDOF resistance level to prevent respectively Collapse ($LF = 1.0$) (Figures 66-73)

# AQG Station – FA030 recording – Low-cycle fatigue damage index – $\mu_{mon}$=4

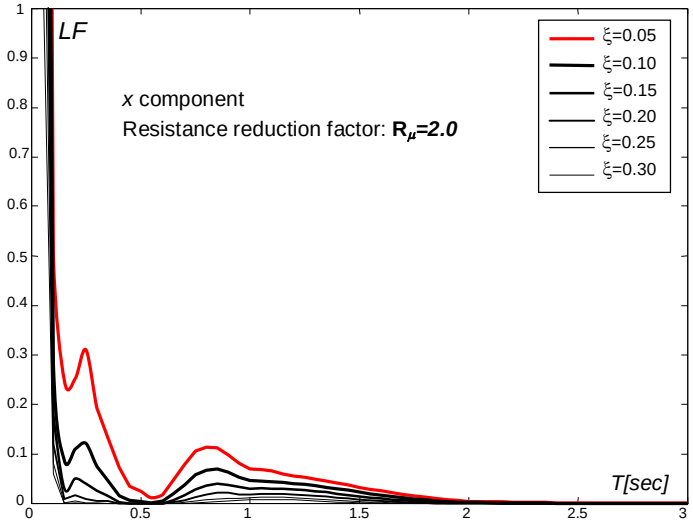


**Figure 42:** *LF* damage index on varying SDOF damping

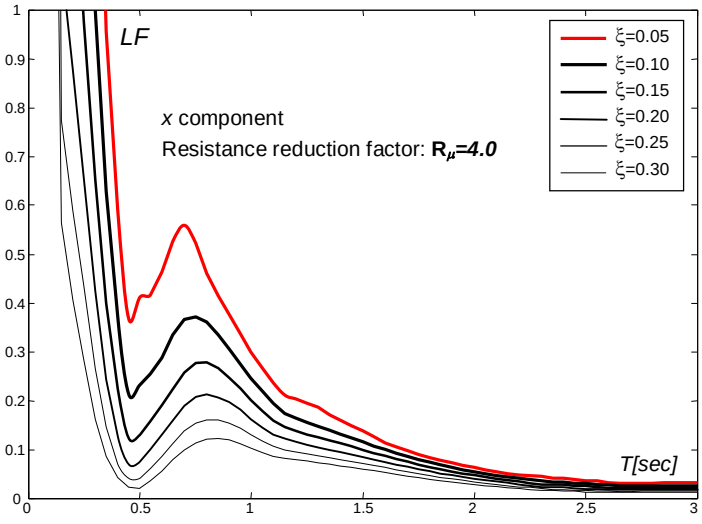


**Figure 43:** *LF* damage index on varying SDOF damping

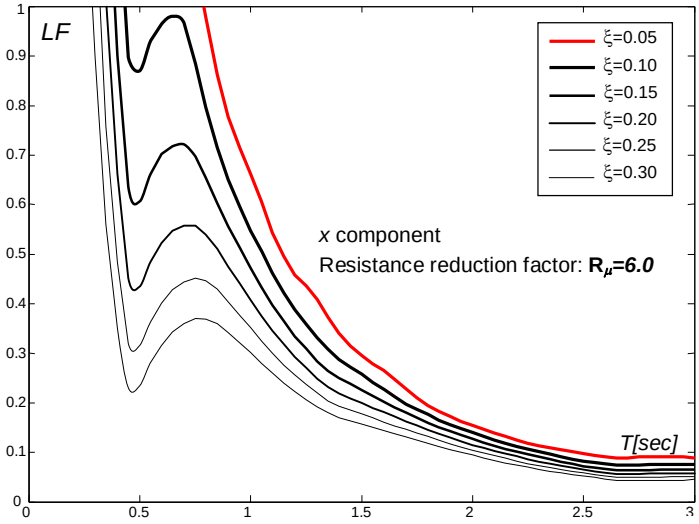


**Figure 44:** *LF* damage index on varying SDOF damping

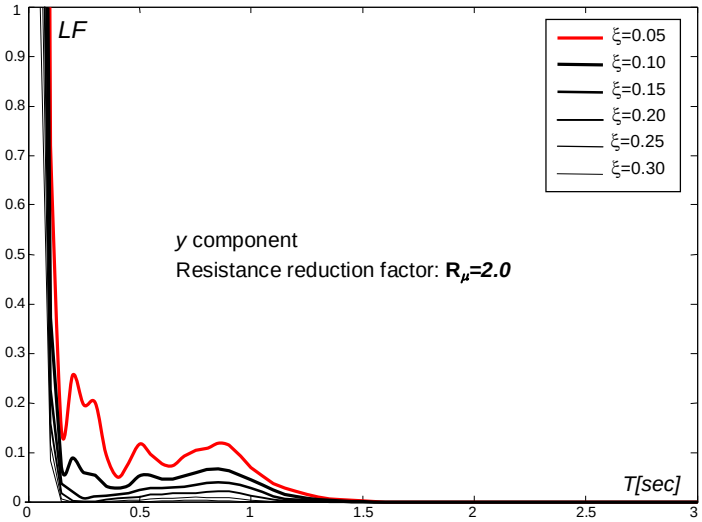


**Figure 45:** *LF* damage index on varying SDOF damping

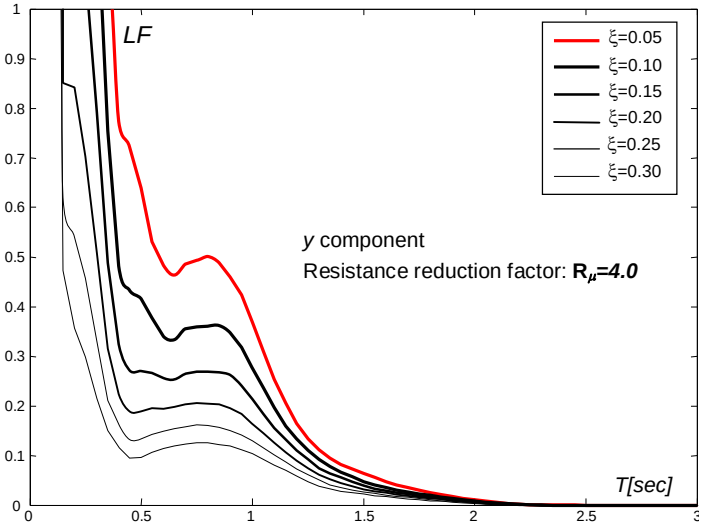


**Figure 46:** *LF* damage index on varying SDOF damping

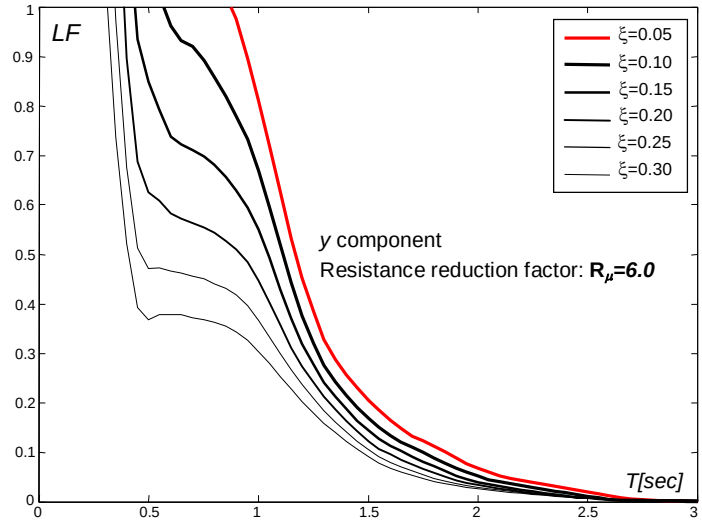


**Figure 47:** *LF* damage index on varying SDOF damping

## *AQX Station – GX066 recording – Low-cycle fatigue damage index – $\mu_{mon}$=4*

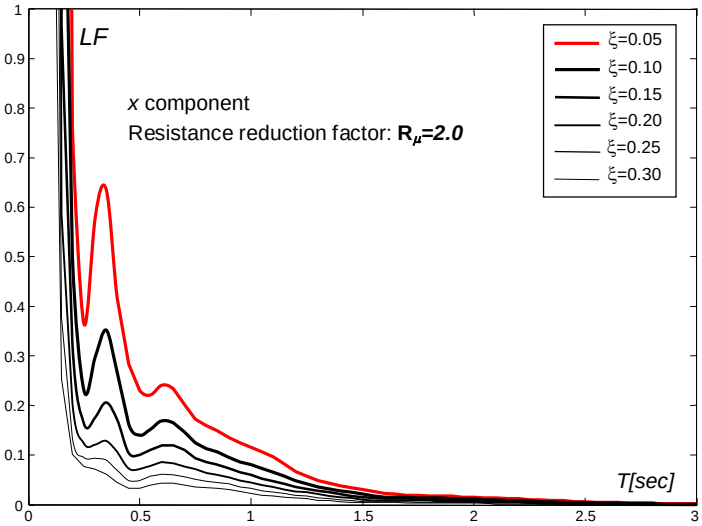


**Figure 48:** *LF* damage index on varying SDOF damping

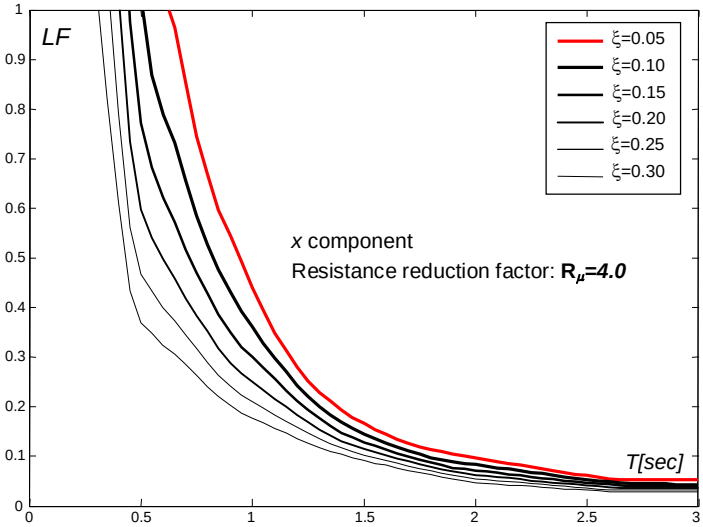


**Figure 49:** *LF* damage index on varying SDOF damping

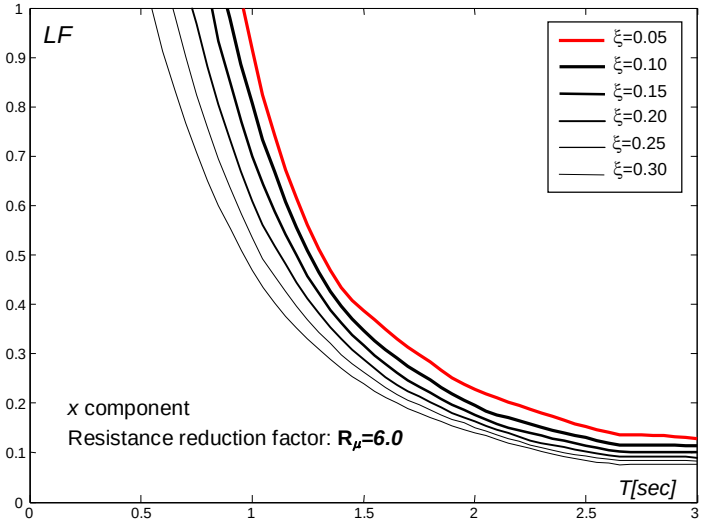


**Figure 50:** *LF* damage index on varying SDOF damping

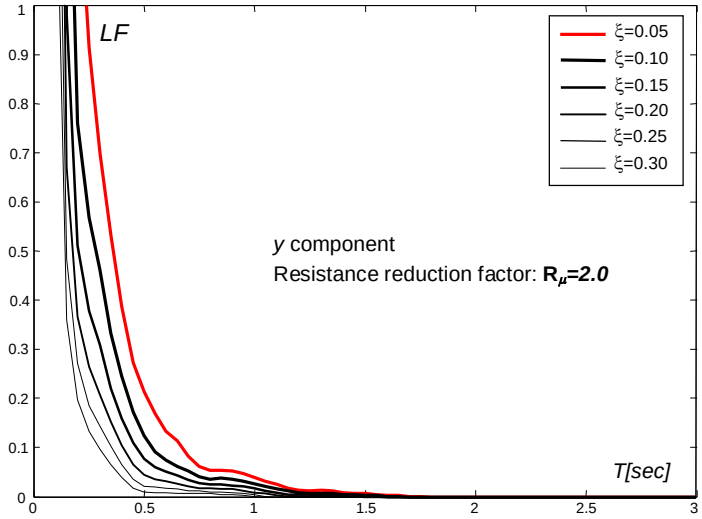


**Figure 51:** *LF* damage index on varying SDOF damping

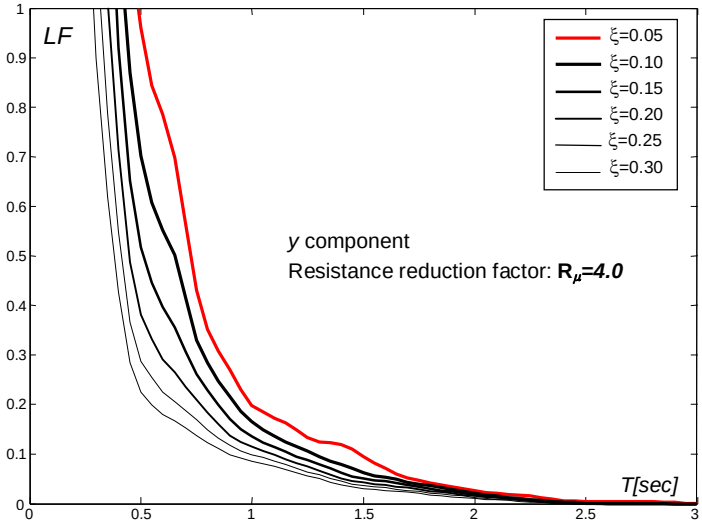


**Figure 52:** *LF* damage index on varying SDOF damping

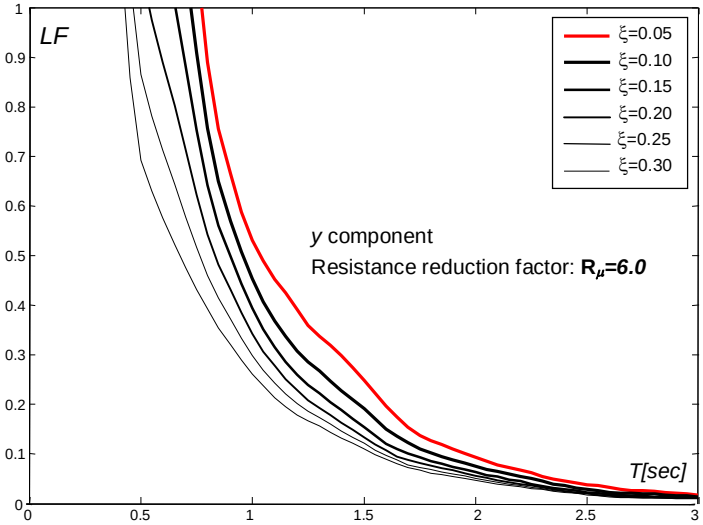


**Figure 53:** *LF* damage index on varying SDOF damping

## *AQK Station – AM043 recording – Low-cycle fatigue damage index – $\mu_{mon}$=4*

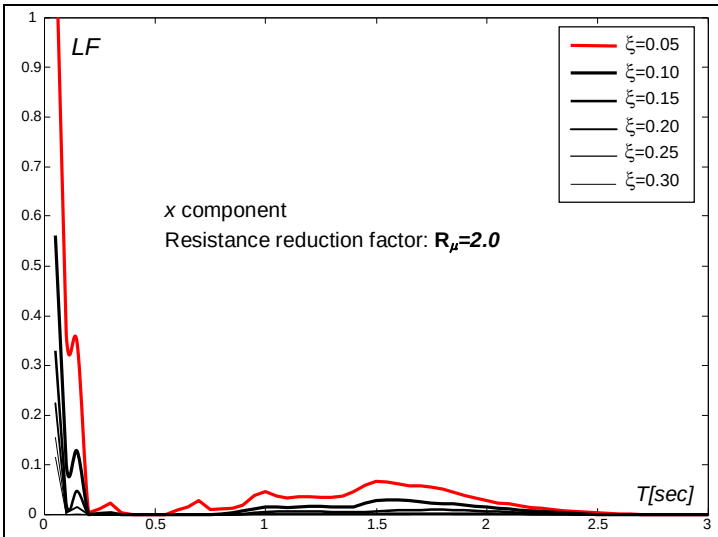


**Figure 54:** *LF* damage index on varying SDOF damping

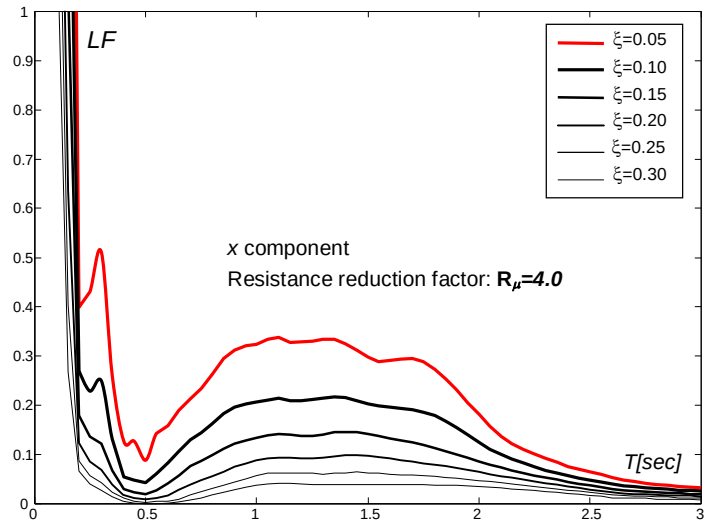


**Figure 55:** *LF* damage index on varying SDOF damping

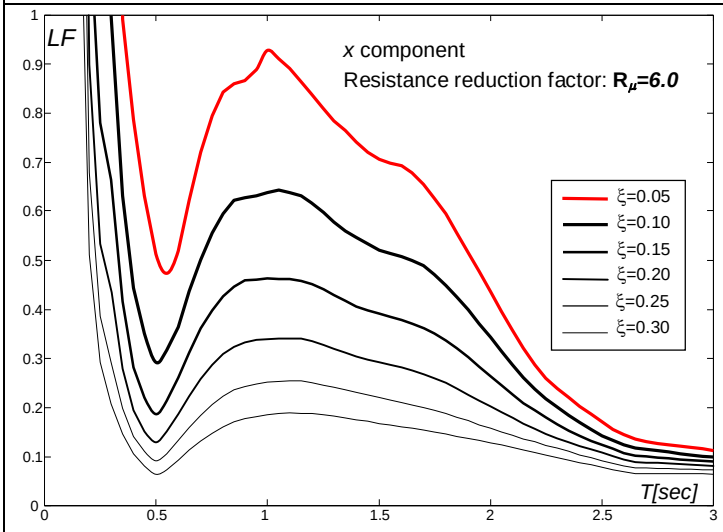


**Figure 56:** *LF* damage index on varying SDOF damping

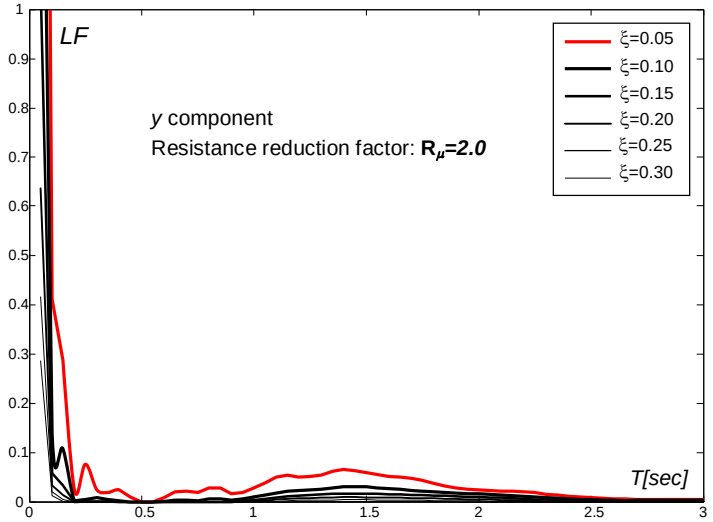


**Figure 57:** *LF* damage index on varying SDOF damping

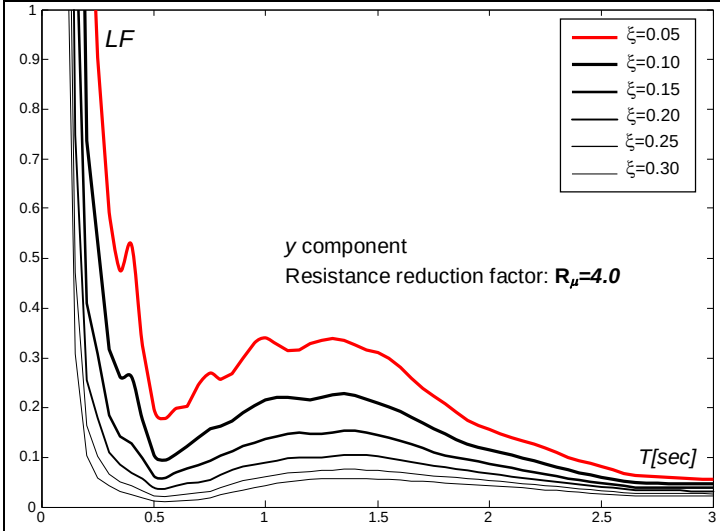


**Figure 58:** *LF* damage index on varying SDOF damping

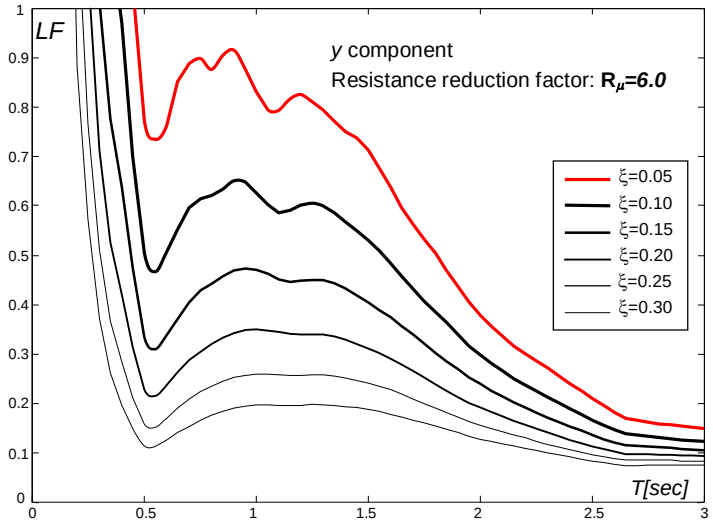


**Figure 59:** *LF* damage index on varying SDOF damping

## *AQA Station – CU104 recording – Low-cycle fatigue damage index – $\mu_{mon}$=4*

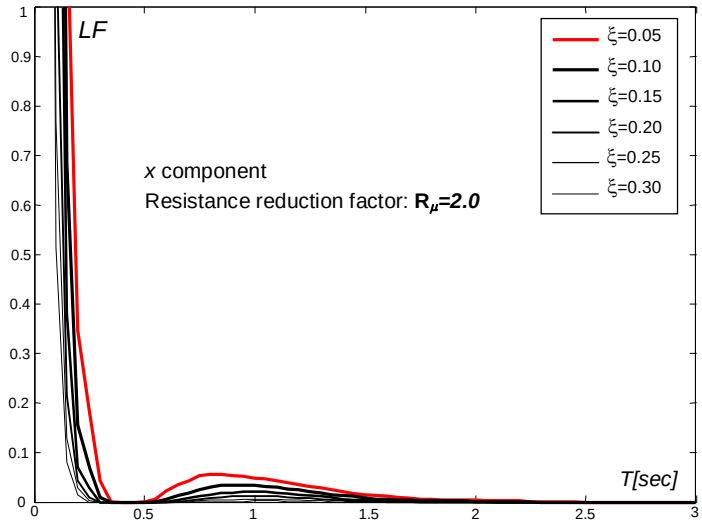


**Figure 60:** *LF* damage index on varying SDOF damping

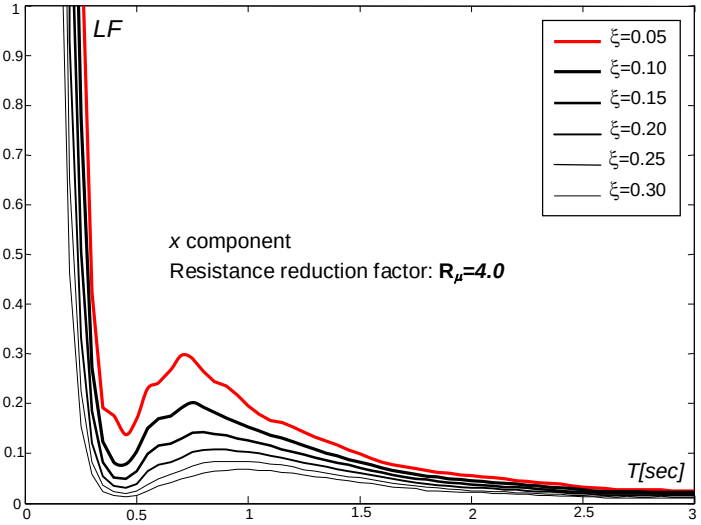


**Figure 61:** *LF* damage index on varying SDOF damping

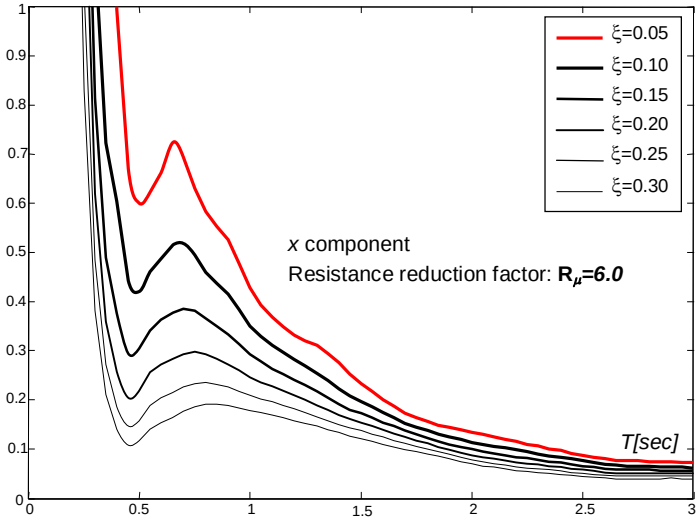


**Figure 62:** *LF* damage index on varying SDOF damping

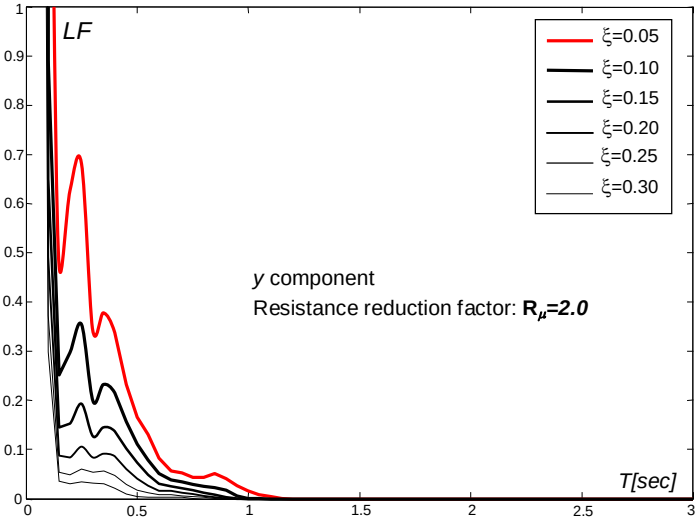


**Figure 63:** *LF* damage index on varying SDOF damping

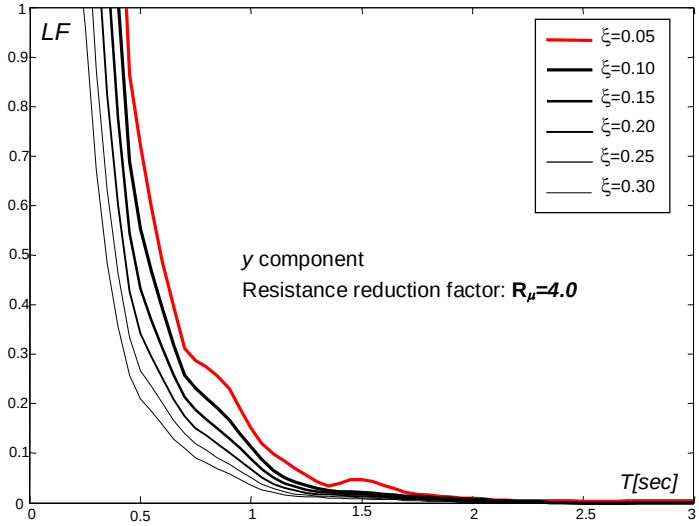


**Figure 64:** *LF* damage index on varying SDOF damping

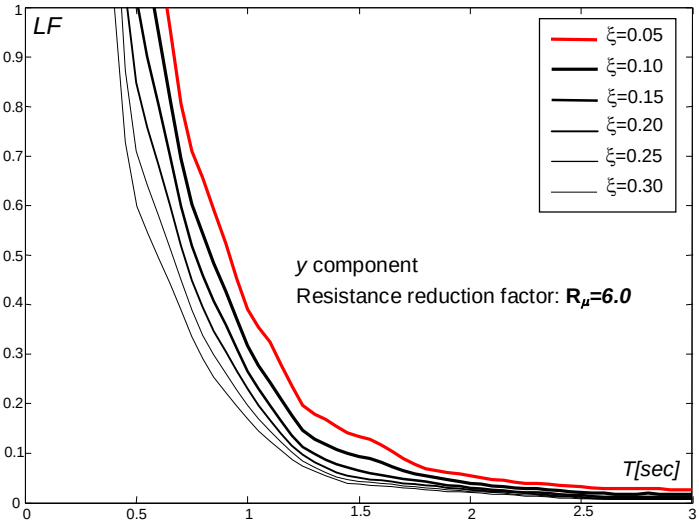


**Figure 65:** *LF* damage index on varying SDOF damping

***AQG Station – FA030 recording – x component***

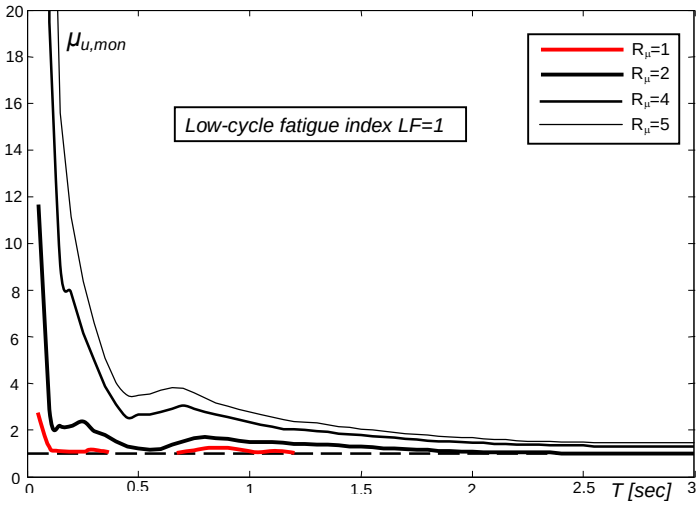


**Figure 66**: Ductility demand spectra for Collapse Limit State (*LF=1.0*)

***AQG Station – FA030 recording – y component***

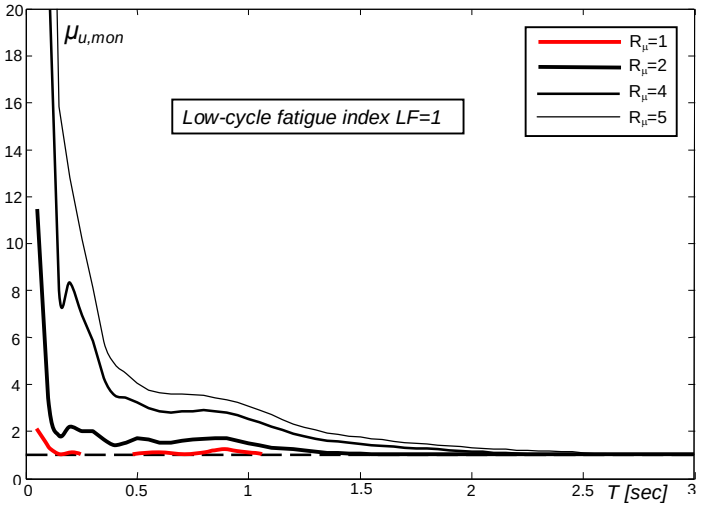


**Figure 67**: Ductility demand spectra for Collapse Limit State (*LF=1.0*)

***AQX Station – GX066 recording – x component***

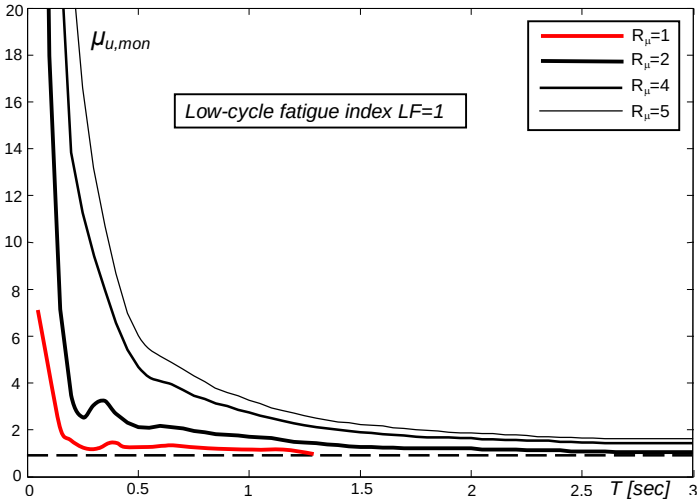


**Figure 68**: Ductility demand spectra for Collapse Limit State (*LF=1.0*)

***AQX Station – GX066 recording – y component***

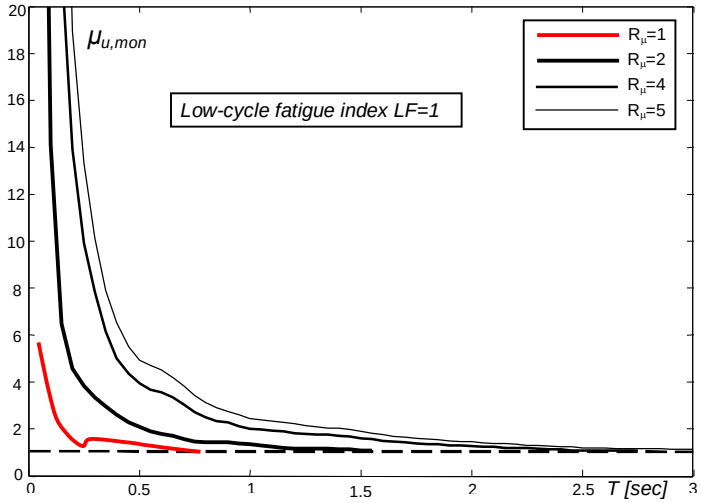


**Figure 69**: Ductility demand spectra for Collapse Limit State (*LF=1.0*)

***AQK Station – AM043 recording – x component***

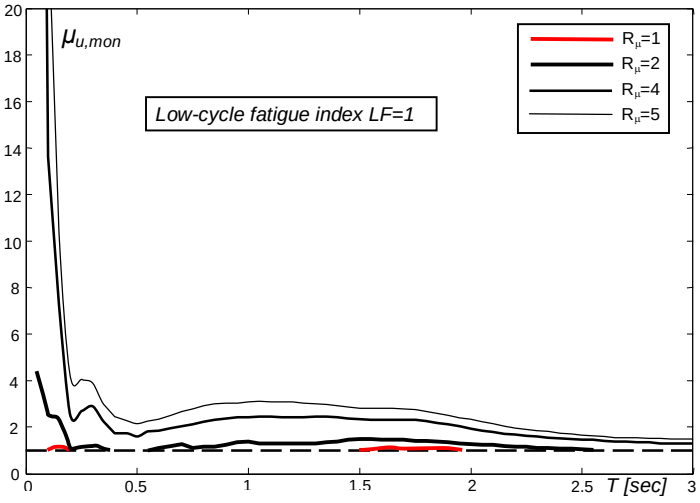


**Figure 70**: Ductility demand spectra for Collapse Limit State (*LF=1.0*)

***AQK Station – AM043 recording – y component***

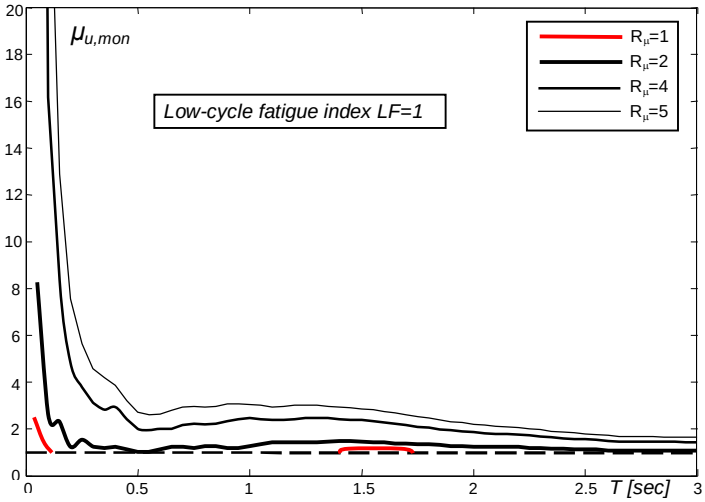


**Figure 71**: Ductility demand spectra for Collapse Limit State (*LF=1.0*)

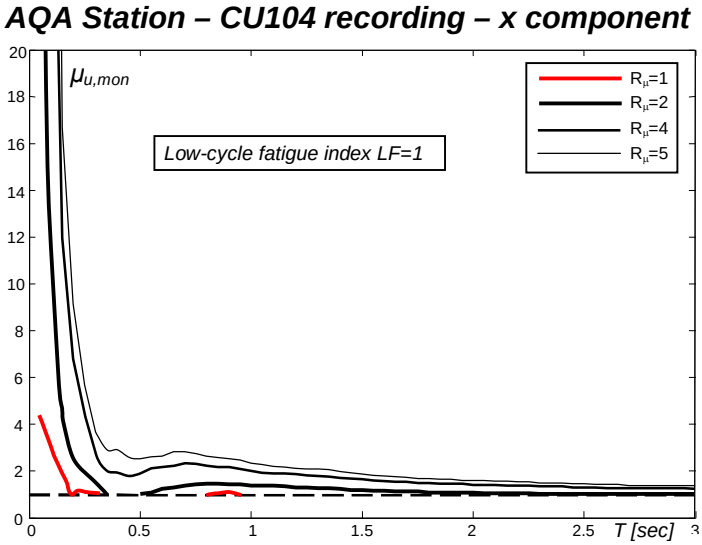


**Figure 72**: Ductility demand spectra for Collapse Limit State (*LF=1.0*)

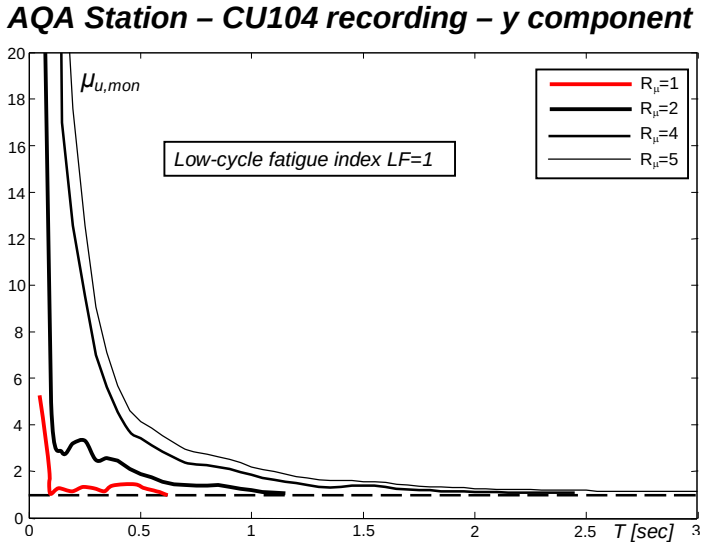


**Figure 73**: Ductility demand spectra for Collapse Limit State (*LF=1.0*)

Obtained numerical results generally confirmed the considerations stated in previous analysis concerning the PA damage index values. In the case of FA030 registration, AQG station, high seismic demand is concentrated in the low period range, moreover a peak in demand is still located within 0.6-0.8 sec. (figure 42-47). The two components of such accelerogram appear to present similar seismic demand. Registration GX066, AQX station, stays as the most dangerous considered excitation, however, the seismic demand, evaluated in terms of *LF* index, presents smoother trend on varying the period if compared with similar results obtained by considering the *PA* index (figure 48-53). This statement can be considered as general, in particular it can be also straightforwardly observed for CU104 registration (figure 60-65). Finally, the increase in seismic demand on high period, iSDOF fundamental period within 1-2 sec, for AM043 registration is confirmed too (figure 54-59).

Results show that *LF* index values are significantly lower than *PA* index for all the considered structural systems, in figure 74-75 comparison between such parameters is plotted for FA030 registration and a pre-assigned iSDOF resistance level for sake of clarity, a similar observation should be extended to every accelerogram and iSDOF took into account. These low values for the fatigue based damage index confirms the impulsive character of the L'Aquila earthquake considered registrations, it's possible, in fact, to define, having fixed the character of the iSDOF displacement seismic demand, for every couple $(\mu_S, \mu_{u,mon})$ a critical value for the number of the plastic cycles can be evaluated (16), if such a value is exceeded LF damage index results higher than PA. Obtained results show *PA>LF* in all the considered cases, which means the seismic accelerograms demands for low number of equivalent cycles on the iSDOF system.

Comparison between the results obtained by using the different adopted damage indexes can be also carried out in terms of their reliability in predicting the observed damage on structures in the area close to the epicentral zone of the considered earthquake registrations. In the light of this, LF index values appear to be more coherent with the real seismic scenario, however the damping effect due to the masonry infills damages and dissipation capacity due to these non structural elements should be carefully taken into account.

Another remarkable aspect, in fact, concerns the role of the viscous damping in reducing the seismic response. As well known, dissipation of energy related to viscous damping is an effective mechanism to improve the seismic performance of a structural system, obtained results for L'Aquila seismic accelerogram confirms this statement proofing the importance of viscous damping capacity in the case of very high seismic demand. In particular a 20% viscous damping coupled with existing building typical ductility resources ($\mu_{u,mon} = 3-4$), should prevent structural collapse or drastically reduce the iSDOF systems set which are going to overtake such limit state (figure 2-25 and 42–65). Such damping level can be practically obtained by retrofit the existing structures with extra-structural dissipation systems, which, in the author's opinion, represent an effective and efficient solution to be considered in order to reduce the seismic risk of existing structures, also when near-fault seismic events have a relevant occurrence probability.

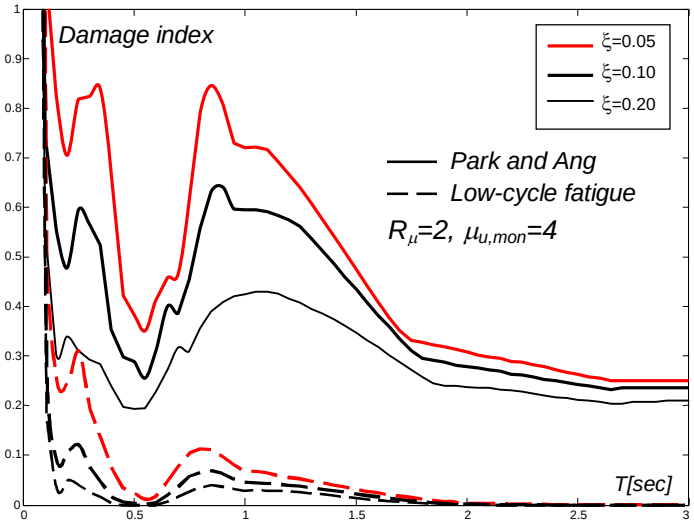


**Figure 74**: Comparison between considered damage indexes – FA030 registration – *x* component

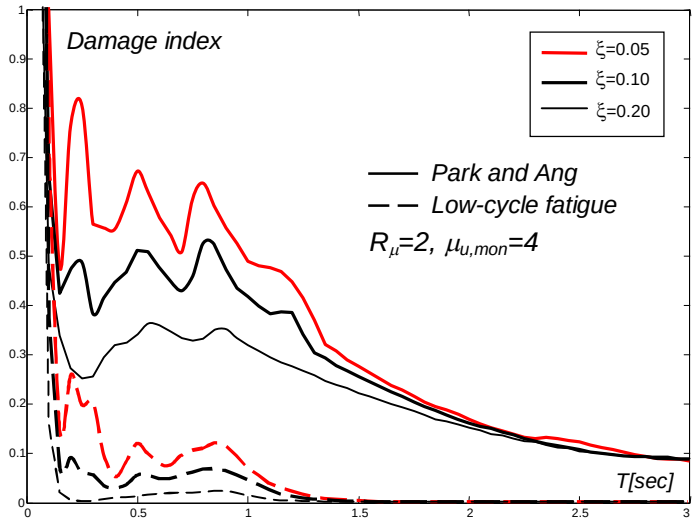


**Figure 75**: Comparison between considered damage indexes – FA030 registration – *x* component

## *CONCLUSION*

In the present report a numerical analysis aiming at evaluating both the Park and Ang (PA) and low-cycle fatigue (LF) damage indexes of iSDOF system having different viscous damping and ductility capacities subject to the four near-fault L'Aquila earthquake registration is presented. Results show how at least two recorded accelerograms (FA030 and GX066) lead iSDOF stiff systems to collapse if NTC 2008 design

provision are applied, proofing the new Italian Code is not able to deal with near-fault seismic components. Furthermore, results obtained with PA index are very much severe than the one from similar analysis carried out by considering the LF index, however the latter appears to be more coherent with the real observed seismic scenario on the site. In this within, more detailed analysis concerning the role played by the masonry infills have to be carried out in order to investigate the reliability of the adopted damage indexes.

Finally, increase of viscous damping appears as an effective way to reduce the seismic damage within the period range in which the seismic excitations present their maximum input energy. This suggests that using extra-structural dissipation systems to retrofit existing structures has to be considered as an effective strategy to reduce the seismic risk also in areas in which near-fault seismic events have a relevant occurrence probability.

***REFERENCES***


(1) L. Petti, I. Marino (2009), Preliminary comparison between response spectra evaluated at close source for L'Aquila earthquake and elastic demand spectra according to new seismic Italian code (v.1.00), available at http://www.reluis.it

(2) ITACA, Italian Accelerometric Archive (http://itaca.mi.ingv.it/ItacaNet)

(3) RAN – National Acceleromteric Network – DPC Dipartimento di Protezione Civile (http://www.protezionecivile.it)

(4) Ufficio sistema informativo geografico – Regione Abruzzo (http://www.regione.abruzzo.it/cartografianew/ )

(5) ACMC (2001) - Level 3 document, "Design for Seismic Action - An example of seismic performance examination for RC building designed according to the Architectural Institute of Japan (AIJ) Guidelines" by YOSHIMURA Manabu and UEDA Tamon.

(6) NTC2008, *Norme tecniche per le costruzioni*, D.M. 14 Gennaio 2008

(7) Park Y.J., Ang A.H., (1985) Mechanistic seismic damage model for reinforced concrete, *ASCE Journal of Structural Engineering*, 111(4): 723-727

(8) Park Y.J., Ang A.H., Wen Y.K. (1987), Damage-limiting aseismic design of buildings, *Earthquake Spectra*, 3(1): 1-26

(9) Kunnath K.S., Hoffmann G., Reinhorn A.M., Mander J.B. (1995), Gravity load designed RC buildings – part I: seismic evaluation of existing constructions, *ACI Structural Journal*, May-June

(10) Kunnath K.S., Hoffmann G., Reinhorn A.M., Mander J.B. (1995), Gravity load designed RC buildings – part II: evaluation of detailing enhancements, *ACI Structural Journal*, July-August

(11) Ingham J.M., Liddel D., Davidson B.J. (2002), An assessment of parameters describing the response of reinforced concrete beam. *Bullettin of the New Zealand society for earthquake engineering* 35, (1)

(12) ATC-40 (1997), Seismic Evaluation and Retrofit of Concrete Buildings. Report No. ATC-40, Applied Technology Council, Redwood City, CA

(13) Coffin L.F. (1954), A study of the effect of the thermal stresses on a ductile metal, Trans. ASME, 76, 931-950.

(14) Manson S.S. (1954), Behaviour of materials under conditions of thermal stress, National Advisory Commission on Aeronautics: Report 1170, Cleveland, Lewis Flight Propulsion Laboratory

(15) Banon H., Biggs J., Irvine H. (1981), Seismic damage in reinforced concrete frames, *ASCE Journal of Structural Engineering*, 107(9): 1713-1728

(16) De Iuliis M., Palazzo B., Castaldo P. (2010), A comparative study between literature seismic damage indexes, to be submitted to *Computer and Structures*